

Title:

FROM THE PAST TO THE FUTURE: SPATIO-TEMPORAL DYNAMICS OF WATER-BALANCE IN A RAPIDLY URBANIZING KATHMANDU VALLEY WATERSHED OF NEPAL

Authors:

- 1) Suchana Acharya, (acharyasuchana@gmail.com)
-Department of Water Resources and Irrigation, Nepal
-Department of Urban Management, Kyoto University, Japan
- 2) Tomoharu Hori (hori.tomoharu.3w@kyoto-u.ac.jp)
-Disaster Prevention Research Institute, Kyoto, Japan
- 3) Saroj Karki (sarojioe@gmail.com)
-Ministry of Physical Infrastructure Development, Province 1, Nepal
-Smartphones for Water (S4W), Lalitpur, Nepal

STATEMENT

This manuscript is a non-peer reviewed preprint. The manuscript has not been submitted to any journal yet.

Twitter

@imeander_

1 **FROM THE PAST TO THE FUTURE: SPATIO-TEMPORAL DYNAMICS OF**
2 **WATER-BALANCE IN A RAPIDLY URBANIZING KATHMANDU VALLEY**
3 **WATERSHED OF NEPAL**

4
5 Suchana Acharya^{1,2}, Tomoharu Hori³, Saroj Karki^{4,5}

6
7 ¹Department of Water Resources and Irrigation, Government of Nepal

8 ²Department of Urban Management, Kyoto University, Japan

9 ³Disaster Prevention Research Institute, Kyoto University, Japan

10 ⁴Ministry of Physical Infrastructure Development, Province-1, Province Government, Nepal

11 ⁵Smartphones for Water (S4W), Lalitpur, Nepal

12
13
14
15 **ABSTRACT**

16 The resources of the earth are under immense pressure due to the multiple anthropogenic
17 influences. The land resources which largely attribute to the quality as well as quantity of the
18 water, is facing extreme stress due to the rapid urbanization resulting from population growth
19 as well as socio-economic development. It is imperative that the response of hydrological
20 processes to the change in landuse is properly understood for the sustainable management of
21 water and land resources. In view of the underlying problem of unscientific landuse practice as
22 a result of the rapid urbanization and the consequent water-stress, this study has attempted to
23 assess the spatio-temporal dynamics of the water-balance components in Kathmandu valley
24 watershed from the past to the future. Forecasting the future landuse scenario and applying
25 popular semi-distributed, physically based hydrological model Soil and Water Assessment Tool
26 (SWAT), the change in water-balance component in the past, present and future scenario was
27 evaluated. In order to exclusively quantify the impact of landuse change, the same climatic
28 conditions are forced for all scenarios. Projection of landuse revealed that nearly half of the
29 total area of Kathmandu valley watershed will be covered by built-up zone by the year 2040.
30 The increase in the built-up area is compensated mainly by agriculture areas and the forest areas
31 which will have further implications on the multiple ecosystem services. The results and
32 analysis clearly indicated that the rapid urbanization will significantly alter the water-balance
33 components of the study watershed that is already reeling under the water-stress. It was also
34 concluded that the impact of landuse change on the water availability will be felt greater at the
35 sub-basin level than at the basin level. The findings of this study entail the urgency to regulate
36 the landuse practice as well as formulate appropriate measures to abate the adverse impacts.

37
38 **Keywords:** Kathmandu Valley, Urbanization, Landuse change, Water-balance, Soil and Water
39 Assessment Tool (SWAT), Hydrological modeling

40 1. INTRODUCTION

41 Water is an indispensable resource for human existence whose sustainability hinges on the
42 balance among the different socio-environmental components. There is no argument over the
43 fact that the stress on this priceless resource is being ever increasing due to the multiple climatic
44 and anthropogenic influences. The alteration of the hydrological cycle that governs the spatio-
45 temporal availability of water is apparent due to the human interference with the natural system.
46 Among different components of the natural system, land resource is one of the key elements
47 controlling the quantity and quality of water resources. Management of landuse, however, has
48 been a major challenge across the globe. The need to accommodate the growing population,
49 particularly in urban areas, has resulted in unplanned and unscientific landuse development
50 which have cascading effect across multiple socio-environmental services. Population
51 projections has estimated about 68% of the world's population to live in urban areas by 2050
52 (United Nations, 2018). Unsurprisingly, migration of people to urban centers is an obvious
53 choice owing to the better economic opportunities especially in developing countries. Driven
54 by such rapid migration and population growth, the landuse in urban areas are transforming
55 alarmingly without due consideration of the future consequences. It is ubiquitous that the
56 landuse landcover (LULC) changes are major driving forces attributing to environmental
57 changes across all spatial and temporal scales (Gashaw et al., 2018). Water, a key ecosystem
58 component, already under severe stress is further expected to aggravate due to the urbanization-
59 triggered rapid and haphazard LULC changes. One of the most important socio-economic
60 processes for establishing far-reaching and long-term ecological effects is land use
61 transformation, especially the human-induced variety termed 'urbanization.' Management and
62 protection of available water resources is a key to sustainable development of human kind.
63 Addressing these issues requires information about the factors that drive hydrological changes
64 and their related effects on local water resources (Aboelnour et al., 2019). Several studies have
65 indicated that the LULC change associated with rapid urbanization impacts the ecosystem by
66 altering the hydrological balance of a watershed (Fang et al., 2020). The urbanization process
67 is transforming permeable land surfaces into impervious surfaces and ultimately changing
68 regional hydrological characteristics (Zhou et al., 2013). The change in LULC can influence
69 watershed hydrology by altering the rates of interception, infiltration, evapotranspiration, and
70 groundwater recharge that result in changes to the timing and amounts of surface and river
71 runoff (Baker and Miller, 2013). According to Wu et al., (2015), LULC changes due to
72 urbanization and deforestation alters the hydrological processes and lead to change of flood

73 frequency and annual mean discharge by impacting the evapotranspiration, soil infiltration
74 capacity, and surface and subsurface flow regimes. Increase in impervious surface areas due to
75 urbanization are responsible for increased runoff, reduced infiltration leading to flash floods
76 and lower groundwater recharge (Ansari et al., 2016; Wakode et al., 2018). Hence for the long-
77 term water-resources planning and management, it is imperative to understand the hydrological
78 response of a watershed to LULC change. In this regard, the appropriate quantification of the
79 change is crucial to formulate mitigation and management plans.

80 Hydrological modelling, in this regard, are widely adopted techniques to understand the
81 catchment hydrological characteristics including the distribution of various water balance
82 components at different level of a watershed. Hydrological models enable understanding and
83 quantification of hydrological processes under the influence of characteristics describing
84 rainfall and catchment features (Kumar et al., 2017). Also, hydrological models are used to
85 perform scenario analysis such as the climate change impact, hydrological response of
86 watershed to LULC change, etc. (Jothityangkoon et al., 2001).

87 In this study, we employed a popular semi-distributed hydrological model Soil and Water
88 Assessment Tool (SWAT) to investigate the impact of landuse change on different hydrological
89 components and the water availability. The future impact on water balance is also quantified
90 after forecasting the future landuse scenario. There have been a number of researches to quantify
91 the impact of LULC on hydrological variables using SWAT model (Kundu et al., 2017; Wagner
92 et al., 2013; Woldesenbet et al., 2017). We chose the Kathmandu valley watershed (KVW)
93 which is one of the rapidly urbanizing area not only in Nepal but in South Asia (Ishtiaque et al.,
94 2017; Muzzini and Aparicio, 2013).

95 Several studies have been conducted previously in the KVW covering varieties of topics related
96 to hydrology and water-resources. A study by Pandey et al. (2010) on Kathmandu valley found
97 that due to urbanization, the groundwater extraction has exceeded the recharge rate by more
98 than twice resulting in consistent depletion of ground water table and recommended for
99 immediate action plans for the sustainable management of groundwater resources. Similarly,
100 Shrestha et al., (2020) analysed the impact of climate change on groundwater resources of KVW
101 under different climate scenarios. Their analysis predicted the decrease in groundwater recharge
102 in future scenario of climate projection. Thapa et al., (2017) applied three different hydrological
103 models to analyse the watershed scale seasonal variation in water-balance components. In the
104 view of severe water deficit in the Kathmandu valley, another study by Thapa et al., (2018)
105 analysed the role of inter-basin water transfer project in bridging the demand-supply gap and
106 hence improving the water-security. Pokhrel (2018) applied Soil and Water Assessment Tool

107 (SWAT) in KVV to quantify the impact of landuse change in the watershed scale water-balance
108 and sediment yield between 2000 and 2010 which showed that the surface runoff has increased
109 while the groundwater discharge has decreased.

110 Each of the previous studies in KVV, however, didn't either consider the LULC in their analysis
111 or didn't make an attempt to forecast future LULC and analyse the future hydrological response
112 of LULC change. Shrestha and Acharya, (2020) analysed the impact of the landuse change on
113 the ecosystem value services of the Kathmandu valley watershed at the basin level. A recent
114 study by Lamichhane and Shakya (2019) analysed the integrated impact of LULC and climate
115 change on the watershed scale water-balance. Their study however didn't analyze the spatio-
116 temporal distribution of water balance at the sub-basin level where the effect of LULC change
117 is more pronounced. Similarly, Lamichhane and Shakya, (2019b) studied the possible alteration
118 in the groundwater recharge zones of KVV due to future LULC changes and revealed that the
119 recharge areas are likely to shrink as a result of the urban expansion. This study however didn't
120 analyse the effect of LULC change on the groundwater availability. Against this backdrop, the
121 current study has made an effort to comprehensively quantify the effect of LULC changes not
122 only from the present to the future but also from the past scenario. The analysis of the impact
123 of LULC change is performed at the sub-basin level which will be more helpful for planners
124 and policy makers in prioritizing the problematic areas for formulating the management plans.
125 The objectives of the current study are to project the future landuse scenario based on the past
126 trends and hence quantify the isolated impact of landuse change on the water-balance
127 components both at the subbasin and the basin level.

128

129

130

131

132

133

134

135

136

137

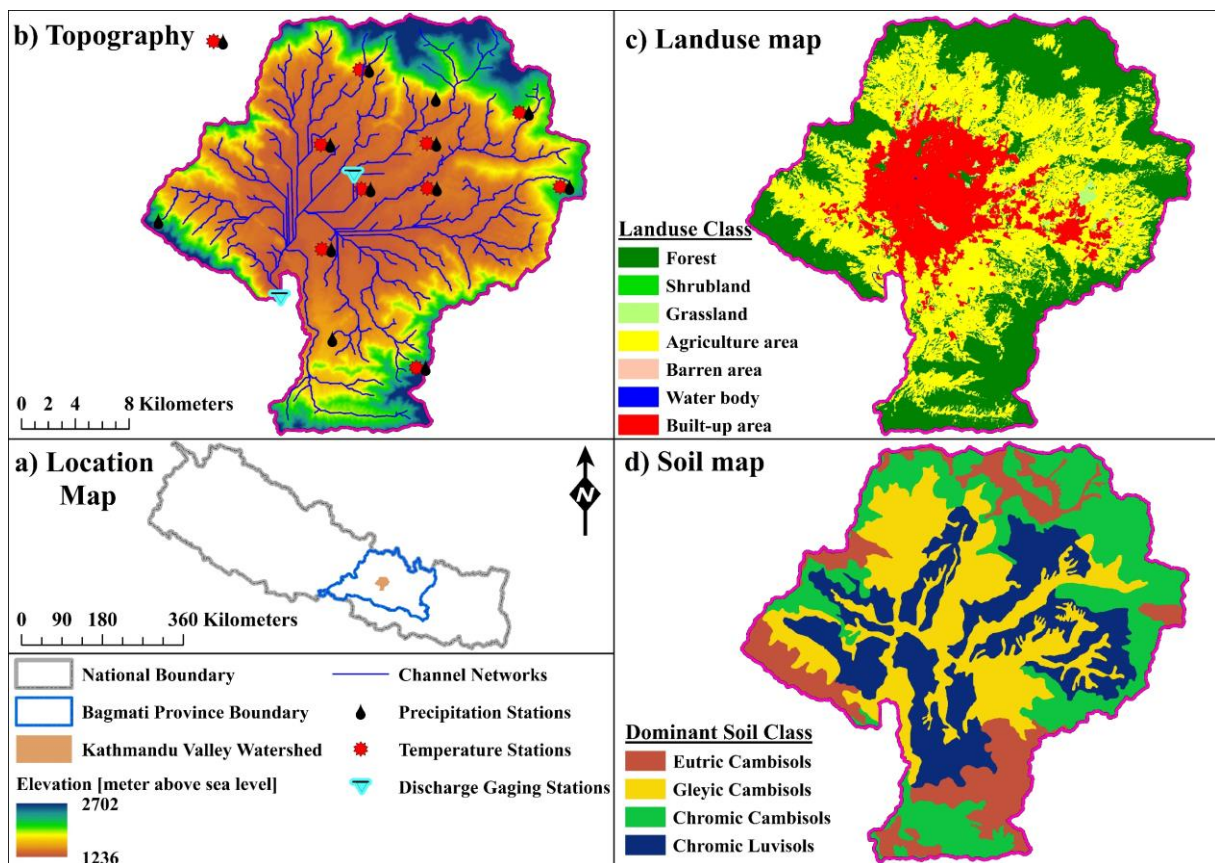
138

139

140

141 **2. STUDY AREA AND THE UNDERLYING PROBLEM**

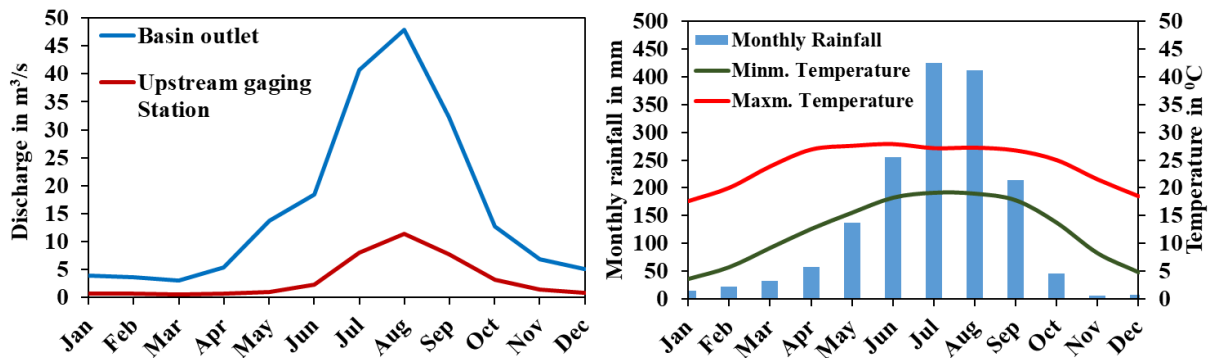
142 The study watershed also known as the Kathmandu valley watershed (KVW) constitutes of
 143 three districts viz. the capital Kathmandu, the historical Bhaktapur and Lalitpur districts within
 144 Bagmati province of Nepal. The valley forms the head water/upstream area of the Bagmati
 145 River basin which stretches to the plains of the Terai before draining to India. **Figure 1 (a-d)**
 146 depicts the location, topography, landuse and the soil types within the KVW. The Bagmati,
 147 typically a rain-fed and partially spring-fed River, drains out KVW originating on the southern
 148 slope of Shivpuri at an elevation of 2700 meter above sea level (masl) (Sharma, 1987). The
 149 KVW surrounded by the forested hills of the Mahabharat range resembles a bowl-shaped valley,
 150 covering an area of 603 km² at the Khokana outlet in Lalitpur district. Forest, agriculture and
 151 the built-up areas are the three major landuse types in KVW (ICIMOD, 2013) whereas the four
 152 dominant soil classes according to the classification of SOTER (Dijkshoorn and Jan Huting,
 153 2009) are eutric cambisols, gleyic cambisols, chromic cambisols and chromic luvisols.



154
 155 **Fig. 1.** a) Location b) Elevation c) Landuse and d) Soil map of the KVW

156 The Kathmandu valley experiences temperate to sub-tropical climate with cold winter and
 157 hot summer where the rainfall is the sole contributor to the water-flow in the basin. Based on
 158 the observed data from the Department of Hydrology and Meteorology (DHM), Nepal for the

159 period 1990-2018, the average annual rainfall in KVW varies between 1600-1800mm of which
 160 over 80% occurs in the monsoon period that typically lasts mid-June to late September. This
 161 signifies considerable spatio-temporal variation in the rainfall pattern.



162
 163 **Figure 2.** Inter-annual variation of a) streamflow and b) Rainfall and Temperature
 164

165 The monthly variation of rainfall and the mean monthly minimum and maximum temperatures
 166 are presented in Figure 2 (a). As illustrated in Figure 2(b), the long-term mean monthly
 167 discharge at the outlet (Khokana Station) of KVW varies between 3m³/s to 48m³/s where March
 168 and August experience minimum and maximum discharge respectively. The pattern is similar
 169 at the upstream gaging station (Gaurighat, Catchment area=68 Sq. km) where the minimum
 170 discharge of 0.5 m³/s occurs in March and the maximum monthly discharge (11 m³/s) occurs in
 171 August. There is a high variation between the dry and the monsoon period average flow in the
 172 basin. Due to this variation, there is significant water-deficit during the dry period.

173 One of the fastest growing cities of South Asia, Kathmandu valley has witnessed a rapid
 174 upsurge in the population in the last few decades. The period 1990-2010 marked a rapid
 175 urbanization in the history of Kathmandu valley during which the valley inhabitants increased
 176 over two folds from about 1.1 million to 2.5 million (CBS, 2012). Migration of the people from
 177 other districts for administrative, economic, educational and medical purposes being a driving
 178 factor behind this rise. Studies and the population projections have claimed this trend to
 179 continue in the future. Unplanned urbanization and development ensued due to the proliferation
 180 of population has adversely impacted socio-environmental services. Among several sectors, the
 181 unscientific conversion of landuse pattern overtops others with cascading effect on multiple
 182 sectors. The land acts as a recharge medium as well as storage beneath the ground and any shift
 183 in the landuse dynamics is certain to alter the quality and quantity of water availability. As it
 184 will be discussed later, the haphazard conversion of forest and agriculture areas into settlements
 185 has put further stress on already deteriorating water-resources of the KKW with dire

186 consequences.

187 The people of the valley are facing acute shortage of water-supply for daily consumption.
188 With growing population, the daily household water demand has grown to nearly 400 million
189 litre per day (MLD). But, Kathmandu Upatyaka Khanepani Limited (KUKL), a government
190 entity managing Kathmandu's water supply, is able to fulfil just about 120 MLD in wet season
191 while a meagre 73 MLD in dry season (Bhusal, 2019). To meet this deficit, people are forced
192 to rely on the private tanker industry. The unregulated and unscientific extraction of
193 groundwater by the tanker industries have led to the severe depletion of groundwater table.
194 Furthermore, due to the rapid extension of residential areas, the groundwater recharge zones
195 have shrunk. On the other hand, the encroachment of the floodplain and drainage area due to
196 the construction of buildings and roads have risen the risks of inundation during monsoon as
197 evident from regular flooding in various parts of the KVW in the recent years. If the current
198 trend continues, the situation will get bad to worse. Sustainable water management approach
199 could be the solution to the water-crisis in Kathmandu valley.

200 3. MATERIALS AND METHODS

201 3.1 Hydro-meteorological and geographical data

202 Hydro-meteorological time series as an input forcing to the hydrological model used in
203 this study includes mean daily discharge, daily rainfall, mean daily maximum and minimum
204 temperatures, relative humidity, solar radiation and the wind speed. Except solar radiation and
205 wind speed, all the above-mentioned dataset was obtained from the Department of Hydrology
206 and meteorology (DHM), Government of Nepal which is the mandate organization for hydro-
207 meteorological measurements in Nepal. The spatial distribution of the different stations
208 covering the study area is indicated in **Figure 1 (b)**. A 30m*30m resolution ASTER (Advanced
209 Spaceborne Thermal Emission and Reflection Radiometer) digital elevation model (DEM) was
210 used for catchment delineation and the extraction of various catchment attributes like stream
211 networks, slope, etc. A soil map that defines the physical properties of soil layers was acquired
212 from the Soil and Terrain (SOTER) database of Food and Agriculture Organization (FAO).
213 Raster layers of the land-use and land cover were obtained from the International Center for
214 Integrated Mountain Development (ICIMOD, [http res.icimod.org](http://res.icimod.org)) for both the period of 1990
215 and 2010. The details on different datasets used in the current study are presented in **Table 3.1**.

216

217

218 **Table 1** Details on the data used for the study

Input data	No. of stations	Resolution	Time Period	Source
Climate				
Rainfall	13	Daily	1990-2000	DHM, Nepal
Temperature	10	Daily	1990-2000	DHM, Nepal
Relative Humidity	5	Daily	1990-2000	DHM, Nepal
Solar Radiation	1	Daily	1990-2000	CFSR-NCEP
Wind Speed	1	Daily	1990-2000	CFSR-NCEP
Hydrology				
Discharge	2	Daily	1990-2000	DHM, Nepal
Geographical				
DEM		30m		ASTER
Soil		1:1000000		SOTER-FAO
Landuse		30m	1990 & 2010	ICIMOD-Nepal

219

220 3.2 Landuse change Prediction

221 The projection of future landuse was performed using Land Change Modeler (LCM) tool
 222 within Terrset software package (<https://clarklabs.org/terrset/land-change-modeler/>). The
 223 prediction of future landuse in LCM is based on the historical landuse change between time 1
 224 and 2. Landuse prediction in LCM is an empirically driven process which moves stepwise from
 225 1) Change analysis 2) Transitional potential modeling and finally 3) the change prediction
 226 (Eastman, 2016). LCM employs a multiperceptron neural network built on the Markov chain
 227 modelling method with cellular automata (CA) (Sinha and Eldho, 2018). The CA-Markov
 228 model is one of the commonly used models among many LULC modelling tools and techniques,
 229 which models both spatial and temporal changes. CA-Markov model combines cellular
 230 automata and Markov chain to predict the LULCC trends and characteristics over time.
 231 Moreover, the CA-Markov model is one of the planning supports tools for analysis of temporal
 232 changes and spatial distribution of LULC (Hamad et al., 2018). There have been a number of
 233 analysis on past landuse change and future landuse prediction using the LCM tools, for example
 234 (Hamad et al., 2018; Anand et al., 2018; Sinha and Eldho, 2018), etc.

235 Landuse maps of two different time period is first given as the input for the model. In
 236 change analysis step, the assessment of actual change between time 1 and time 2 is performed.
 237 The quantitative assessment of different LULC categories, net change of each LULC class and
 238 the contributors to the net change experienced by each LULC category are calculated. The
 239 changes in the landuse are the transition from one landuse class to another landuse class. If the

240 study area contains high number of landuse classes, the combination of transitional potential
241 could be very large.

242 3.3 SWAT model set-up, Sensitivity Analysis, Calibration and Validation

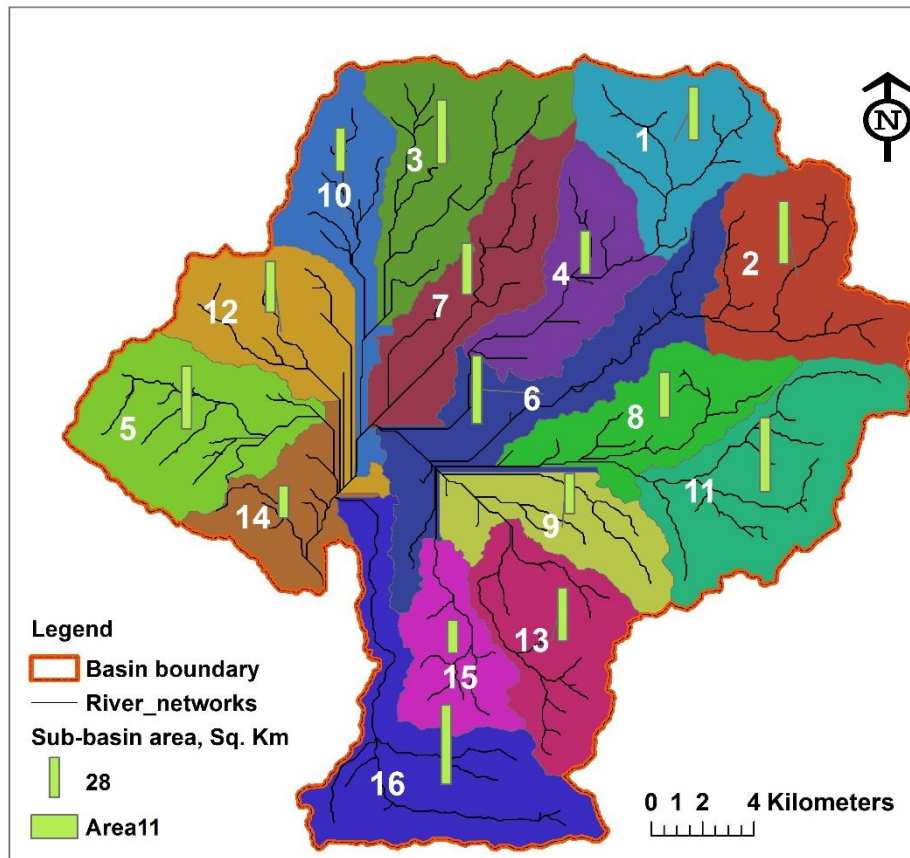
243 Soil and water assessment tool (SWAT) (Arnold et al., 1998) employed in this study is a
244 physically based, continuous time-scale semi-distributed model capable of simulating different
245 physical processes pertaining to the movement of water, sediment, nutrient, crop growth, etc.
246 within a watershed (Neitsch et al., 2011). SWAT model requires information on the climate,
247 hydrology, soil, topography and land use. It allows the impact assessment of management
248 practices and climate on water resources, sediment, and agricultural related processes at
249 watersheds and larger river basins with varying soils, land use, and management conditions over
250 long periods of time (Abbaspour *et al.*, 2007; Winchell *et al.*, 2013). SWAT accounts for the
251 spatial heterogeneity by partitioning of a watershed into different sub-basins and sub-basins
252 further discretized into Hydrological Response Units (HRUs) which are aggregated land areas
253 within a sub-basin comprising unique landuse, soil, slope and management conditions (Neitsch
254 et al., 2011). The study watershed as depicted in Fig. 2 was divided into 16 subbasins and further
255 into 148 HRUs. Land phase of the hydrologic cycle which controls the amount of water,
256 sediment, nutrient and pesticide loadings to the main channel is solved by SWAT model using
257 the following water balance equation:

$$258 \quad SW_t = SW_0 + \sum_{i=1}^t (R_{day} - Q_{surf} - E_a - w_{seep} - Q_{gw})$$

259 Where, SW_t is the soil water content at the end of the day, SW_0 is the initial amount of soil
260 water content, t is the current time in days, R_{day} gives the amount of rainfall in i^{th} day, Q_{surf}
261 indicates the amount of surface runoff on day i , E_a gives the amount of evapotranspiration,
262 w_{seep} gives amount of percolation on day i and Q_{gw} is the amount of return flow on day i . All
263 the components are in mm.

264 The runoff from the daily rainfall was computed based on the modified Soil Conservation
265 Service (SCS) curve number method whereas the Potential evapotranspiration (PET) was
266 estimated using the Penman-Monteith method.

267 SWAT-Calibration and Uncertainty Analysis Program (SWAT-CUP), a stand-alone tool was
268 employed to perform the sensitivity analysis, the calibration and validation of SWAT model.
269 Sensitivity analysis is a procedure of recognizing the most significant parameters for calibration
270 and validation purpose ((Moriassi et al., 2007). Its objective is to evaluate the sensitivity of the
271 model output to the changes in input parameter values particularly when the model consists of



273

274

Fig. 3. Subbasin delineation of the study watershed.

275 consists of the overall procedures performed to achieve the best possible agreement between
276 the simulated and the observed values. The agreement between the observed and the predicted
277 variables are measured statistically based on some goodness-of-fit indicators known as
278 objective functions. In essence, model calibration is a procedure of modifying the model
279 parameters, within their recommended ranges, with an objective of attaining the best possible
280 values of the objective functions. Model validation is performed to assure that the calibrated
281 model properly assesses all the variables and conditions which can affect model results, and
282 demonstrate the ability to predict observations for periods separate from the calibration effort.
283 In this study, the popularly used Nash-Sutcliffe Efficiency (*NSE*) was selected for the model
284 calibration purpose (McCuen et al., 2006). However, additional three objective functions were
285 also assessed for the performance evaluation of the model. Coefficient of Determination (R^2),
286 PBIAS (Gupta *et al.*, 1999; Moriasi et al., 2007) and the Kling-Gupta Efficiency (KGE) (Gupta
287 et al., 2009) were also assessed. Krause *et al.* (2005) reported that R^2 and *NSE* are the most
288 widely used statistics for both calibration and validation.

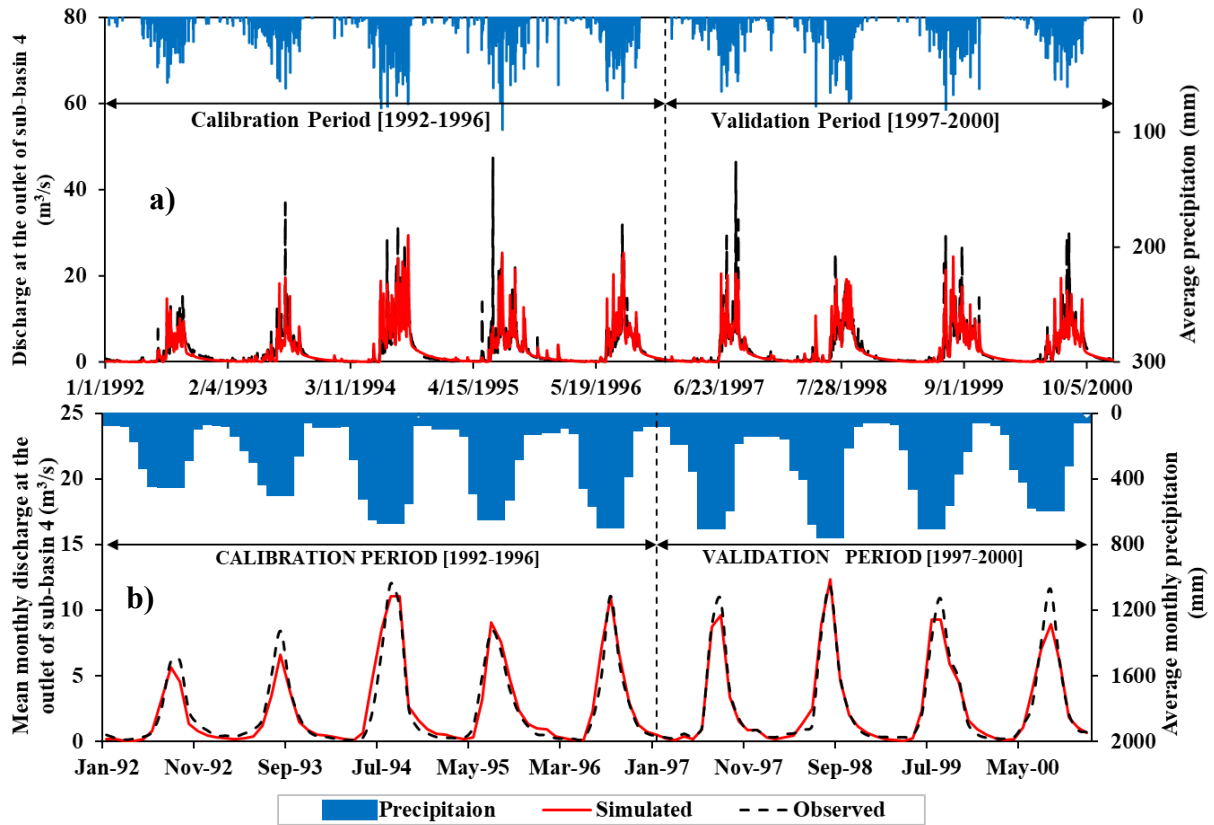
289 The model calibration and validation were executed for the daily discharges but the results were

290 evaluated for the monthly values as well. Two discharge gauging sites, one located at sub-basin
291 4 and the other at the basin outlet, were chosen for calibration and validation purposes. A five-
292 year period [1992-1996] was selected for the calibration while the validation was done for the
293 period 1997-2000. A warm up period of two years [1990-1991] was used for both the sites
294 during the calibration. Warm up period was aimed at stabilizing initial conditions of soil water
295 (Cibin et al., 2010; Kim et al., 2018).

296 **4. Sensitivity Analysis, Calibration and Validation of SWAT model**

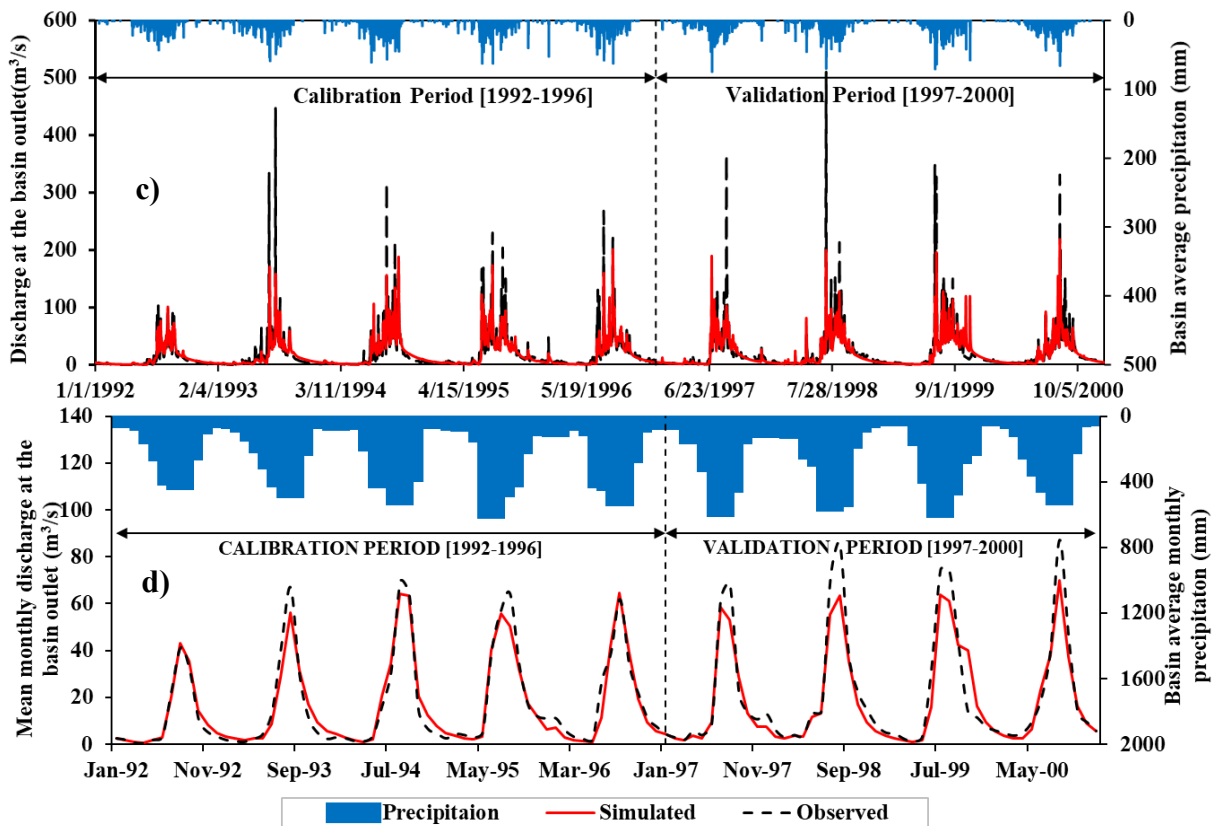
297 The selection of input parameters for this study were based on the previous studies on
298 this watershed (Pokhrel, 2018). The most sensitive parameters are represented by groundwater
299 process, evaporation and surface runoff. It is found that for the study area; SURLAG.bsn,
300 SOL_Z.gw, GW_delay, EPCO.hru, SOL_AWC.sol and REVAPMN.gw were among the most
301 sensitive parameters.

302 The calibration-validation was performed using two gaging stations simultaneously, one at sub-
303 basin 4 (Gaurighat Station) and the other at the outlet of the basin (Khokana Station). The use
304 of multiple sites helps to preserve the spatial heterogeneity of the catchment during parameter
305 calibration. The calibration and validation are basically performed for daily discharge.
306 However, the daily calibrated model was also run for the monthly time step and the performance
307 were evaluated. The comparison of observed and simulated discharge at the two gaging stations
308 as illustrated in **Fig. 4 (a-d)** shows that the model has quite well reproduced the actual condition.
309 However, in some instances, peak flows are underestimated while the low flows are accurately
310 mimicked. For both the stations, the observed and simulated mean monthly flows showed closer
311 resemblance than the daily case for both low as well as peak flows. Similarly, **Fig. 5** depict the
312 scatterplot of observed versus simulated discharge where it can be seen that the flows are in
313 good agreement with each other for both the stations. The comparison of the flow duration curve
314 (FDC) for the calibration and validation period are shown in **Fig.6**. Although FDC is a
315 subjective approach of model evaluation, it gives an important information about the occurrence
316 of flows which are vital in the design and allocation of water-resources projects (Karki, 2012).
317 The overall occurrence of flows was precisely simulated for basin outlet while the low flows
318 were slightly underestimated at subbasin-4.



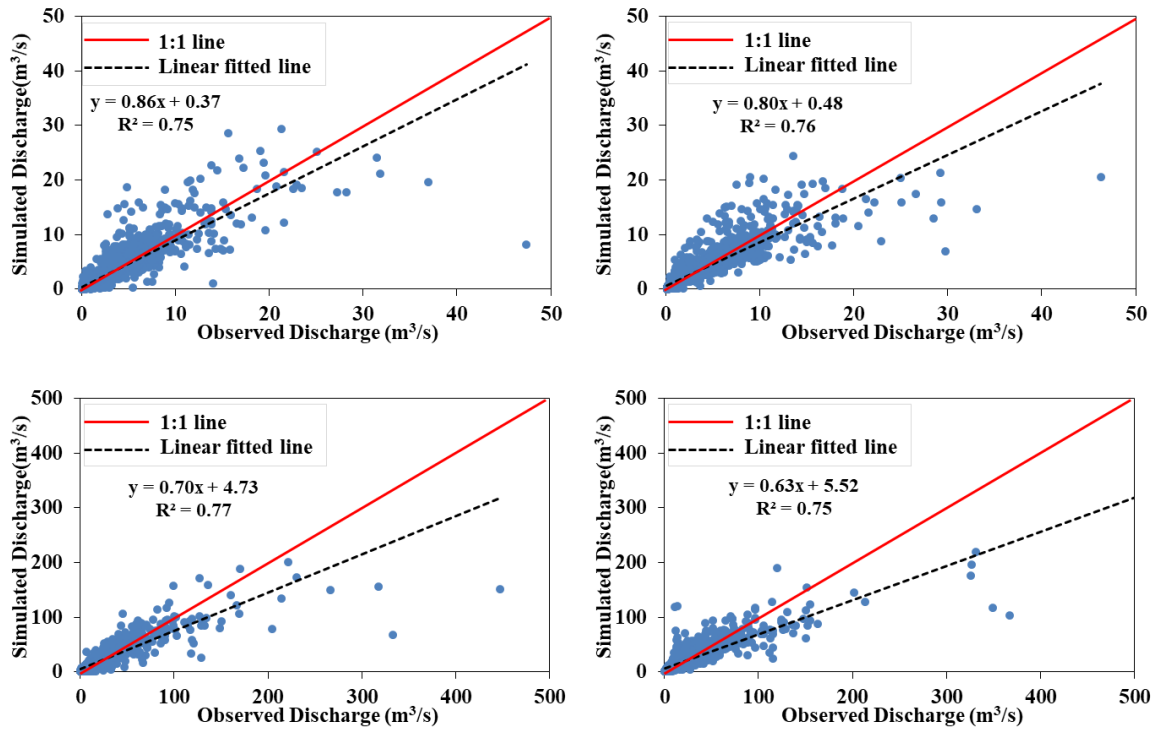
319

320 **Fig.4.** Comparison of observed and simulated discharge at sub-basin 4 a) daily b) monthly



321

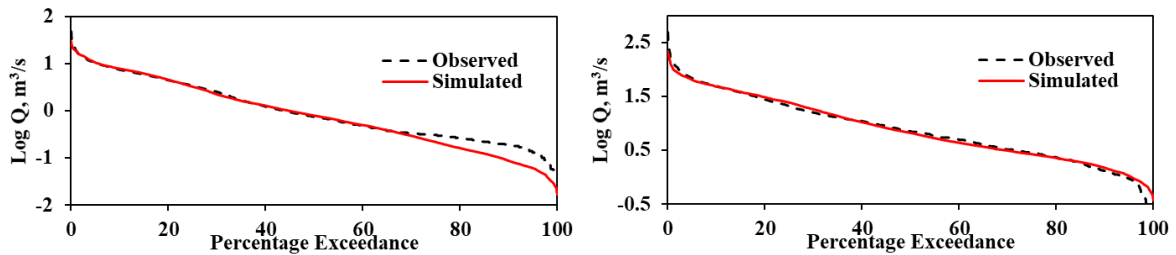
322 **Fig.4.** Comparison of observed and simulated discharge at the basin outlet c) daily d) monthly



323

324

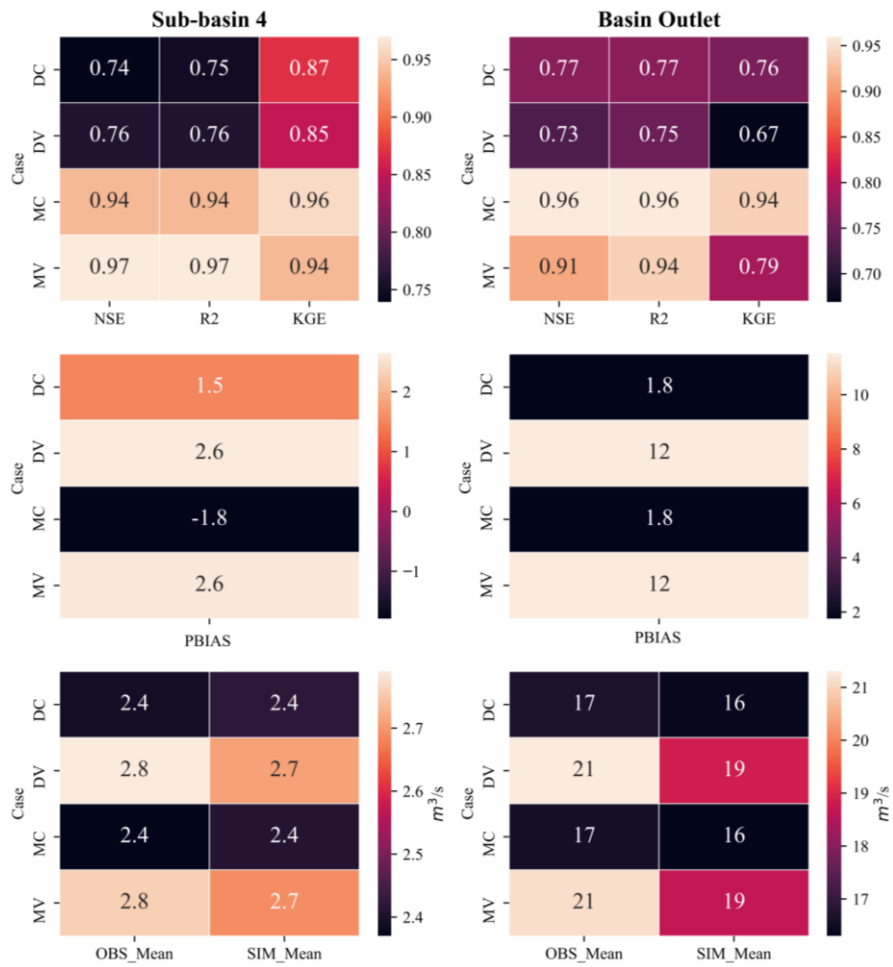
325 **Fig. 5.** Scatterplot of observed vs simulated discharge for subbasin 4 (a) Calibration and b)
 326 Validation and for basin outlet (c) Calibration (d) Validation



327

328 **Fig. 6.** Comparison of observed and simulated flow duration curve during the simulation period
 329 for a) subbasin 4 and b) basin outlet

330 Different model performance indices which portray the accuracy of the predicted results are
 331 presented in **Fig.7.** Each performance indices obtained for both the gaging stations are well
 332 above the satisfactory range as described in Moriasi et al., (2007). The performance indicators
 333 showed further improvement for monthly time-step. Also, the comparison between the observed
 334 and the simulated mean discharge were found to be matched closely.



DC: Daily calibration, DV: Daily Validation

MC: Monthly calibration, MV: Monthly Validation

Fig. 7. Performance evaluation of SWAT model based on different objective functions [Right column represents basin outlet while left column represents Sub-basin 4]

335

336

337

338

339

340

341

342

343

344

345

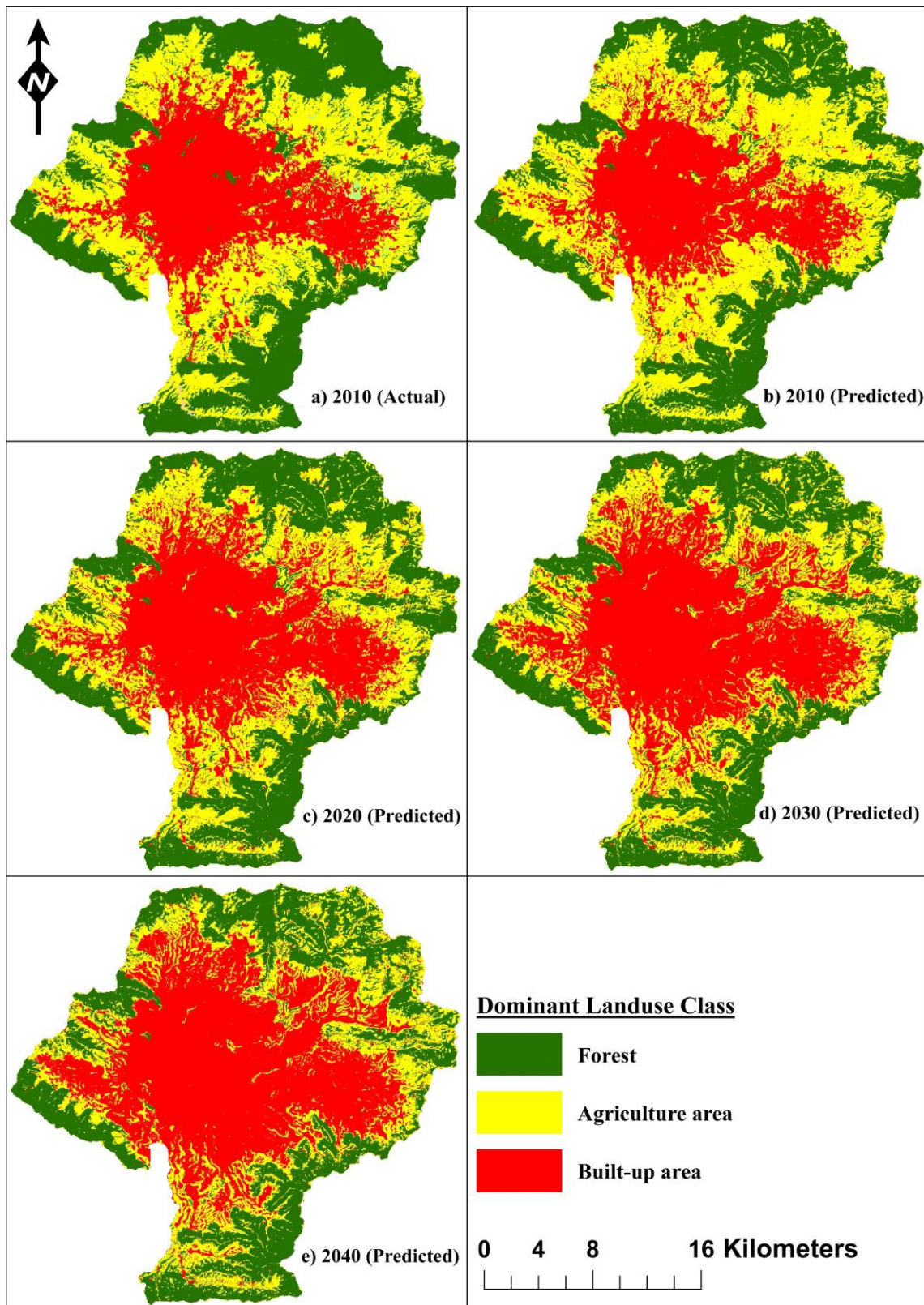
346

347

348

349 5. RESULTS AND DISCUSSIONS

350 5.1 Landuse change prediction

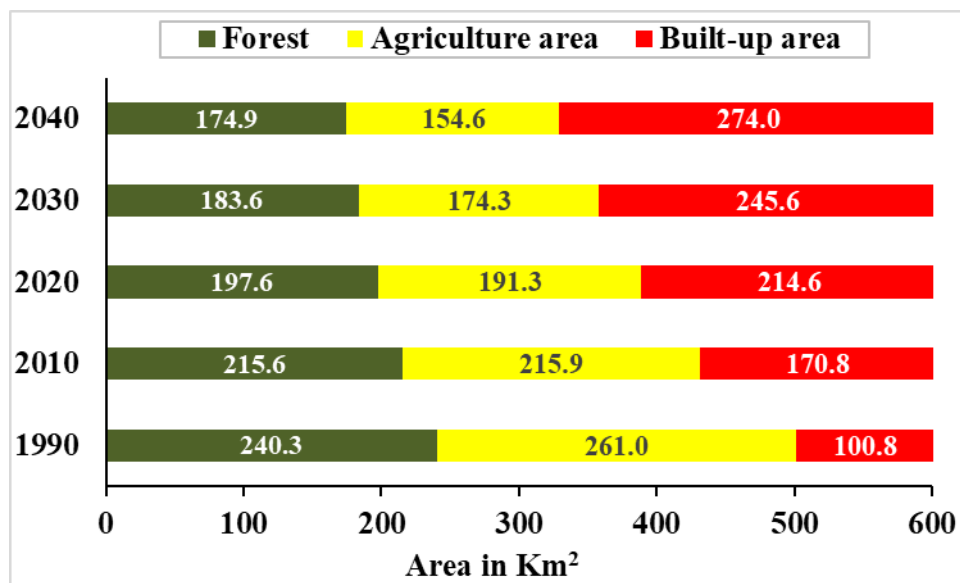


351

352

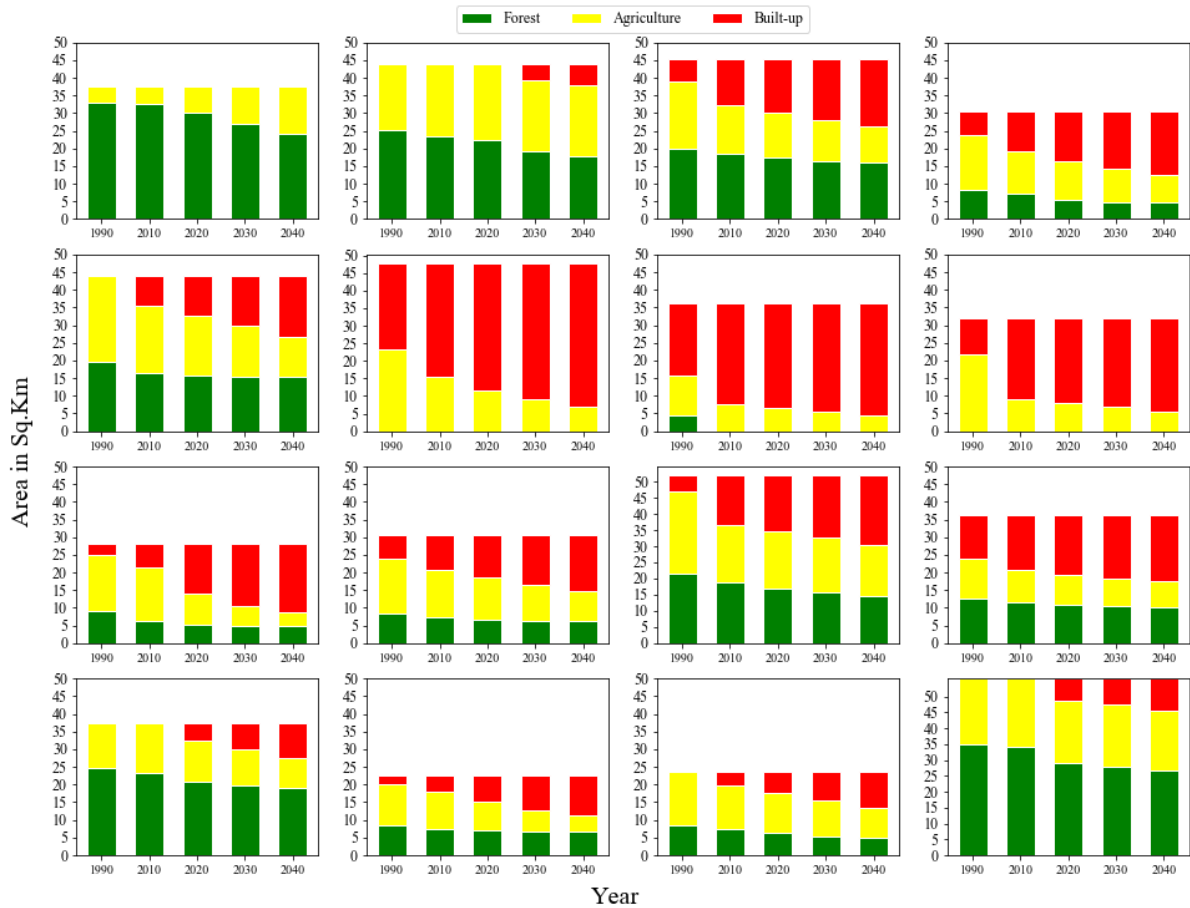
Fig. 8. Predicted landuse map of KVVW for different years

353 The available landuse map of 1990 and 2000 were used to calibrate the model and hence
 354 forecast the landuse for the year 2010. The available landuse map of 2010 and the predicted
 355 map of 2010 as illustrated in **Fig.8, a** and **b** respectively were compared to confirm the accuracy
 356 of the predicted results. The comparison of actual and predicted landuse of 2010 in **Fig.8**
 357 demonstrate that the spatial distribution of different landuse is predicted quite well. Finally, the
 358 future landuse map of 2020, 2030 and 2040 were projected. Based on the trend of the past
 359 decades, the forest and the agricultural areas are expected to decrease while the built-up areas
 360 indicate rising pattern. The quantification of the landuse for different years are summarized in
 361 **Fig.9**. From 1990 to 2010, the forest cover and agriculture areas decreased by about 25 Sq. km
 362 and 45 Sq. km respectively. This decreased area has been transformed to built-up areas which
 363 increased by approximately 70 Sq. km. This period marks a rapid urbanization period in the
 364 history of the Kathmandu valley. The population of the Kathmandu during this period nearly
 365 increased by 2.5 times from about 1.1 million to 2.5 million. It can be seen in Figure 5.8 that
 366 the forest areas in 2040 will reduce to approximately 175 Sq. km from 216 Sq. km in 2010.
 367 Similarly, the agriculture areas will decrease by about 60 Sq. km to 155 Sq. km in between
 368 2010-2040. The forest and agriculture areas combined contributed to more than 80% of the total
 369 catchment in 1990. However, it is expected that this will reduce to about 55% of the total
 370 catchment area. In the same period, the percentage of built-up areas will increase from 17% to
 371 nearly half of the total catchment area. This change in the landuse can have a profound effect
 372 on the overall water-balance scenario of the basin.
 373 Based on the projection, nearly 50% of the total area of the KVW will be covered by built-up
 374 areas by 2040 which is more than 250% of the baseline period of 1990.



375
 376

Fig. 9. Change in dominant landuse classes in KVW from 1990 to 2040

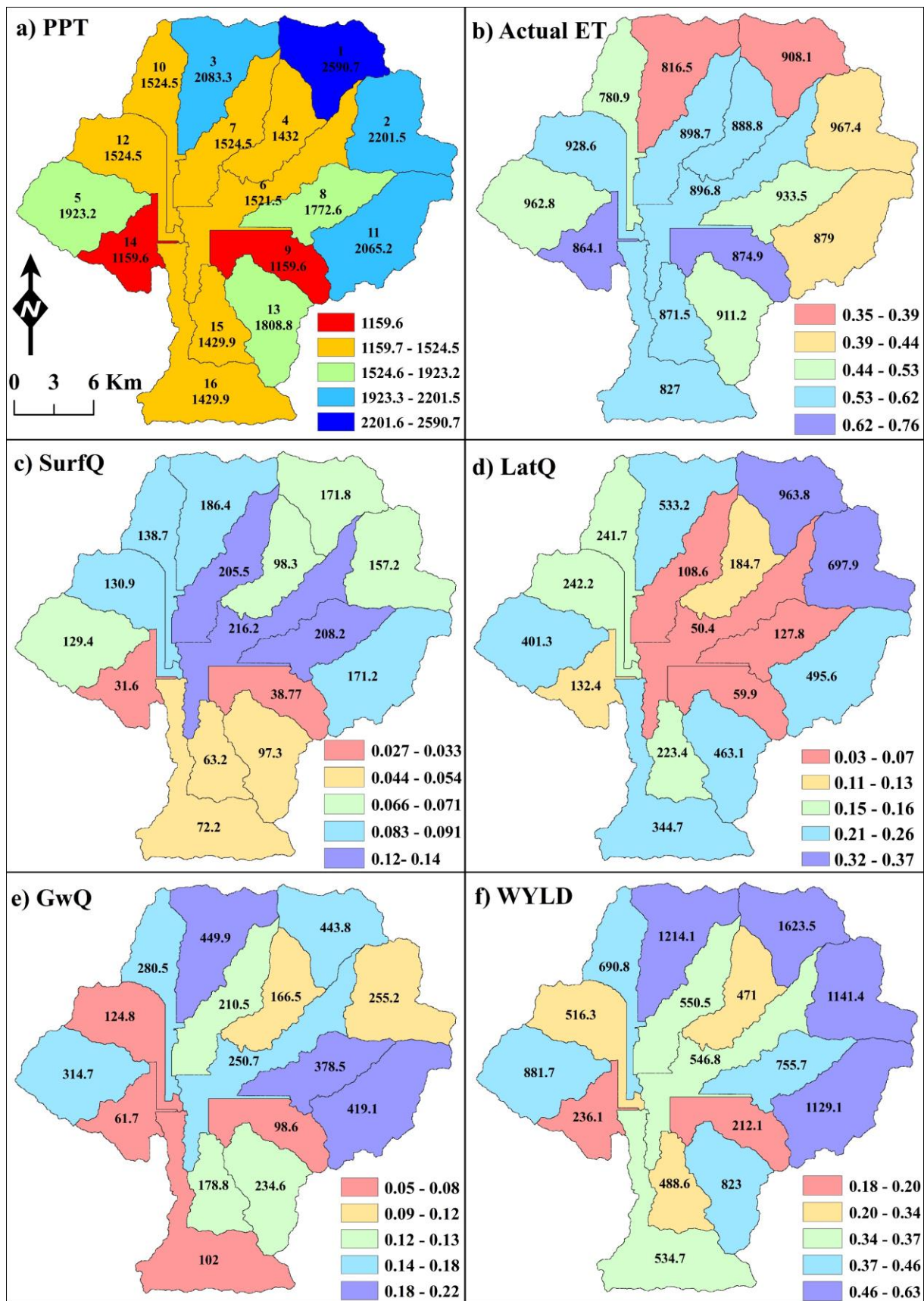


377
 378 **Fig. 10.** Change in the landuse in different sub-basins within KVV
 379

380 5.2 Analysis of water-balance

381 5.2.1 Water-balance under the past landuse of 1990 (the baseline scenario)

382 The validated model was run for the period 1990-2000 (1990-91: two years warm-up period)
 383 under the landuse of 1990 and the climate data of the same period. This case is considered as
 384 the baseline scenario in this study. Based on the simulated results, different water-balance
 385 components were quantified both at the sub-basin as well as basin level. **Fig. 11** illustrate the
 386 spatial distribution of different water-balance components at the sub-basin level of KVV. In
 387 **Fig. 11(a)**, the two labels (top and bottom) inside the map represent the sub-basin number and
 388 the mean annual precipitation (in mm) respectively. The spatial distribution of mean annual
 389 precipitation in different subbasins as shown in **Fig. 11(a)** indicate the considerable variability
 390 within the KVV. The difference between the least rainfall receiving subbasin to the most rainfall
 391 receiving subbasins is more than double of the least value. During the simulation period, the
 392 mean annual precipitation ranged from below 1200mm to above 2500mm and is generally
 393 higher for north-eastern (upper) and lesser for south-western (lower) subbasins. In the **Fig.11(b-**



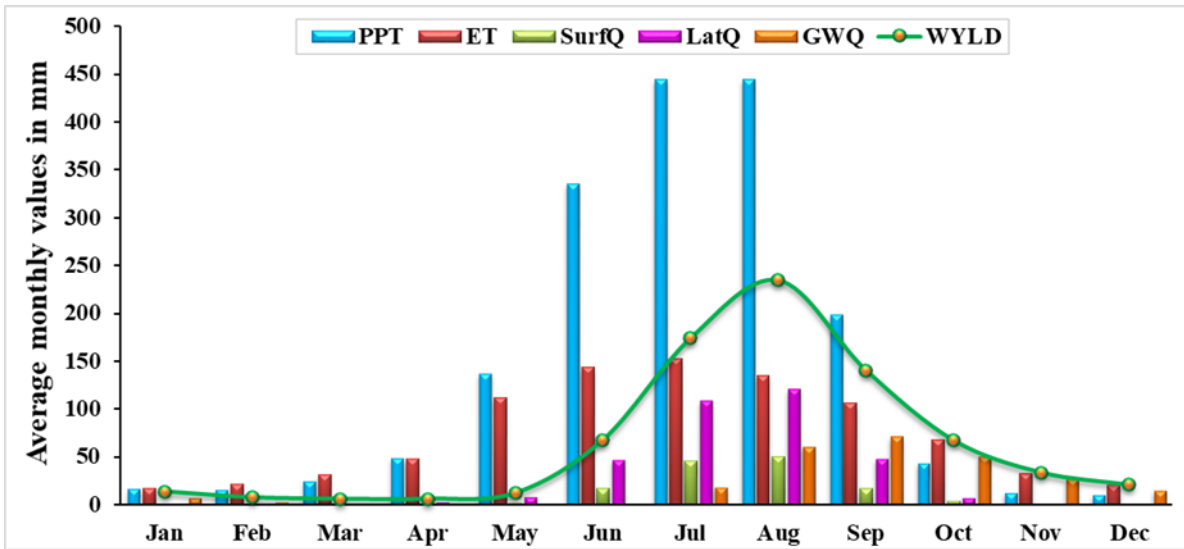
394 **Fig. 11.** Spatial distribution of different water-balance components at the subbasin level under
 395 1990 landuse conditions (baseline scenario)

396 **f)**, the value labelled in the map represent the actual values while the values of the colour-bar
397 indicate the values normalized by annual rainfall of the respective subbasins. These color-bar
398 therefore depicts different water balance components as a fraction of the mean annual
399 precipitation of the corresponding sub-basins.

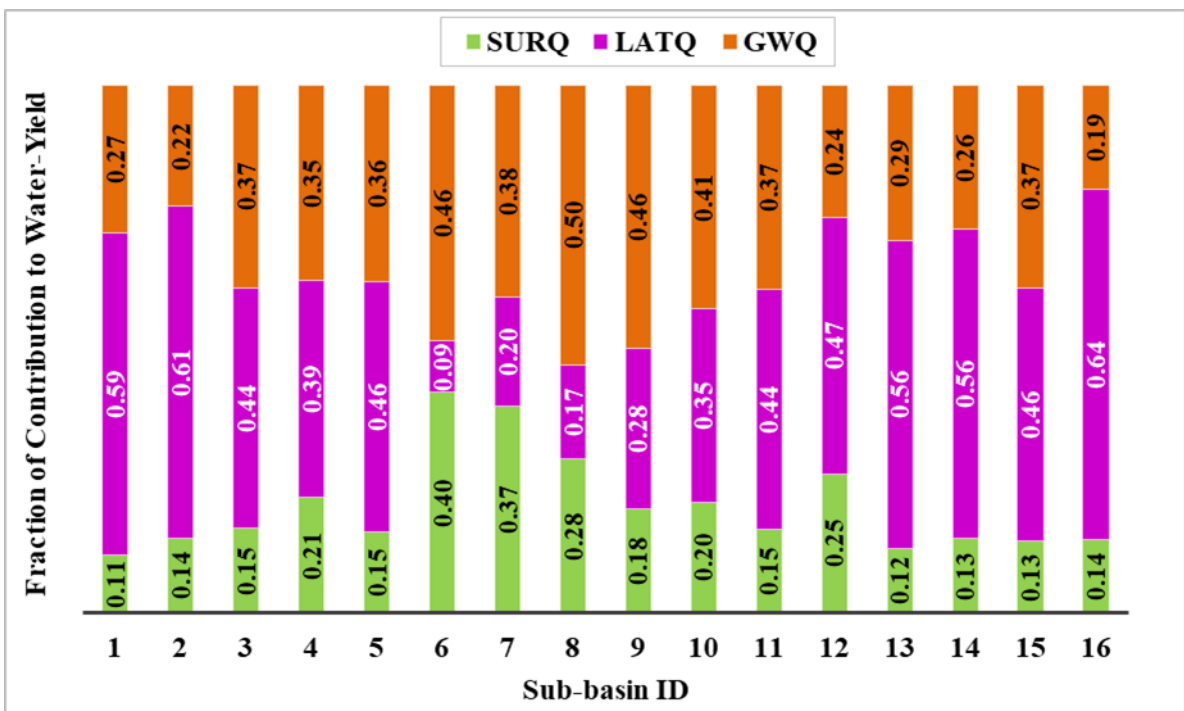
400 According to **Fig.11(b)**, the actual ET, in general, was found to be higher for forest and
401 agriculture dominated subbasins like 1, 2, 5, 8,12, 13, etc. The annual rainfall values in these
402 subbasins are also relatively higher. However, the fraction of the rainfall lost as ET was higher
403 for subbasins like 4, 6, 7, 9, 12, 14, 15, 16, etc. Most of such subbasins are built-up area
404 dominated. The surface run-off is mainly influenced by the impervious cover of the landuse i.e.,
405 built-up area as well as the amount of precipitation. In relation to this, the surface runoff
406 component (SurfQ), as expected, was observed to be higher for built-up areas dominated
407 subbasins like 6, 7 and 8 as depicted in **Fig.11(c)**. The higher values of surface run-off
408 component in other subbasins like 1, 2, 3 and 11 is attributed to the greater rainfall and steeper
409 slopes in these subbasins. Also, the fraction of precipitation transformed to surface run-off is
410 greater in built-up areas dominated subbasins 6 and 7. Similarly, the lateral flow (LatQ) is
411 generally smaller for these subbasins whereas its contribution is higher in forest and agriculture
412 dominated subbasins as shown in **Fig.11(d)**. The groundwater component is also mainly
413 controlled by the land cover type and the amount of annual precipitation. It was observed that
414 the highest groundwater discharge occurred in forest and agriculture dominated sub-basins like
415 1, 3, 5, 8, 10 and 11. Similarly, the least groundwater discharge was observed in sub-basin 9,
416 12, 14 and 16. However, the distribution of lateral Q showed that it was least in sub-basin 6, 9
417 including 4, 7, 8 and 14. The distribution of average annual water yield for each sub-basin is
418 illustrated in **Fig.11(f)**. Water yield is generally higher in subbasins with higher precipitation as
419 well as forest dominated sub-basins like 1-3, 5, 8, 11 and 13. The water yield of different
420 subbasins varied between 212mm to 1623mm with an average value of 784mm for the KVW.
421 8 out of 16 subbasins of KVW were found to have below-average water-yield. Also, it can be
422 deduced that the subbasins surrounding the KVW results in greater water yield than those
423 located at the valley floor.

424 The intra-annual (monthly) variation of different water-balance components including the
425 water-yield has been illustrated in **Fig.12** which signifies a high temporal variation in the water-
426 balance components. Water yield is below 50mm from October to April and increases between
427 May to September as contributed by the precipitation in these months. The relative contribution
428 of surface run-off, lateral Q and the groundwater Q to the total water yield for each subbasins
429 has been demonstrated in **Fig.13**. The contribution of surface run-off to total water yield is

430 higher for subbasins 6, 7 and 8 whereas the contribution of GwQ and LatQ is higher for other
 431 subbasins. The contribution of surface runoff to the water yield varied between 0.11 in subbasin
 432 1 to 0.4 in subbasin 6. Similarly, the contribution of lateral Q to the water yield varied between
 433 0.09 in subbasin 6 to 0.64 in subbasin 16. On the other hand, the contribution of groundwater
 434 Q to the water yield varied between 0.19 in subbasin 16 to 0.50 in subbasin 8.



435 **Fig. 12.** Intra-annual variation of different water-balance components in KVV

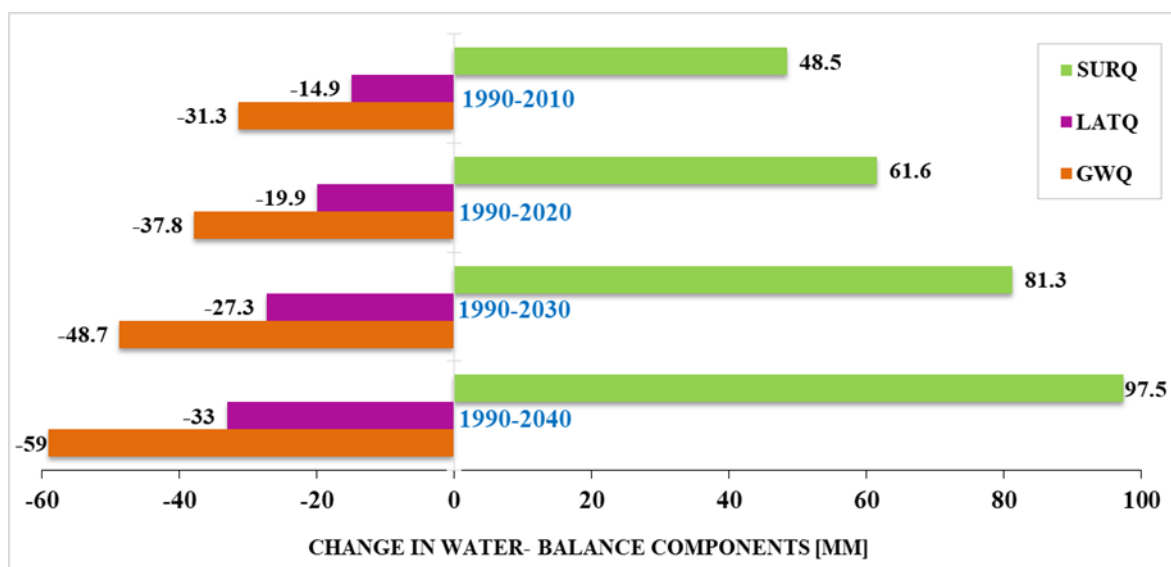


436
 437 **Fig. 13.** Fraction of contribution of water-balance components to water yield in each subbasin
 438 in the KVV.

439 5.2.2 Water-balance change analysis under the present and future landuse at the basin level

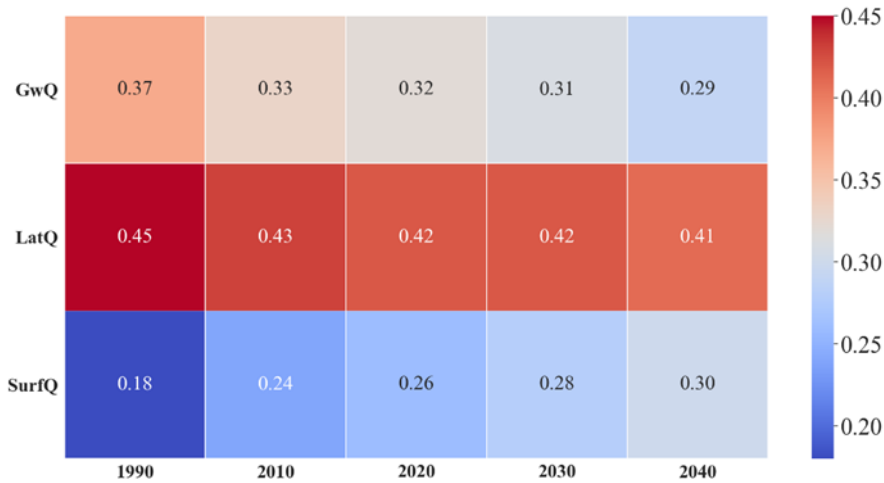
440 The impact of landuse change on different components of water-balance is discussed herein.
441 The average annual water-yield at the basin outlet for the baseline period was 784mm. However,
442 there was no change in the water-yield at the basin outlet for future landuse because the input
443 climate data were the same in all periods. But the impact of landuse was mainly observed in the
444 change in the relative contribution of each components of the water-yield. **Fig.14** illustrates the
445 actual change (+ve or -ve) in different water-balance components relative to the baseline
446 scenario of 1990 landuse at the basin level. Positive values indicate the increase while the
447 negative values suggest the decrease. Surface runoff is expected to increase in the future
448 scenario of 2040 by nearly 100mm of which almost 50% (48mm) increased between 1990 and
449 2010. On the other hand, the lateral Q and groundwater Q showed decreasing trend with future
450 landuse change. Lateral Q decreased by 33mm whereas groundwater Q showed a fall of 59mm
451 between 1990 and 2040. The increase in the urban areas will shrink the recharge zones which
452 will affect the quantity of water entering the aquifer in the sub-surface layer.

453 The percentage contribution of each component to the total water yield at the basin level is
454 shown in **Fig. 15**. The effect of landuse change was more intense on the surface run-off,
455 followed by groundwater and lateral Q. The contribution of surface runoff increased from 18%
456 in 1990 to 30% in 2040. Meanwhile, groundwater contribution to the water yield was 37% in
457 1990 but it is expected to reduce to 29% in 2040. Similarly, the contribution of lateral Q will
458 reduce by nearly 4% from 45 to 41% between 1990 and 2040. The intra-annual variability in
459 the water-balance for different time period at the basin level is illustrated in **Fig. 16**.



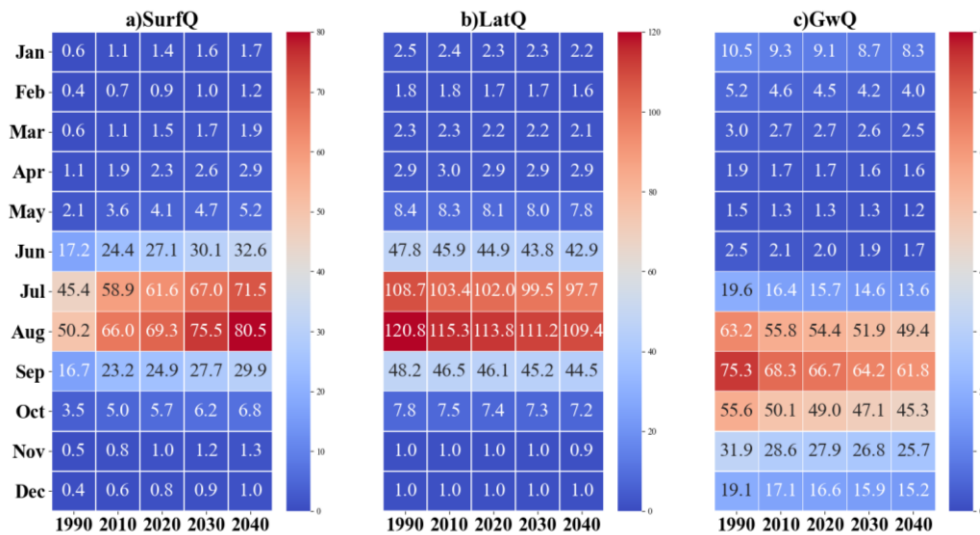
460

461 **Fig. 14.** Projected change in water-balance components with reference to baseline scenario.



462

463 **Fig. 15.** Comparison of relative contribution of water-balance components for different decades



464

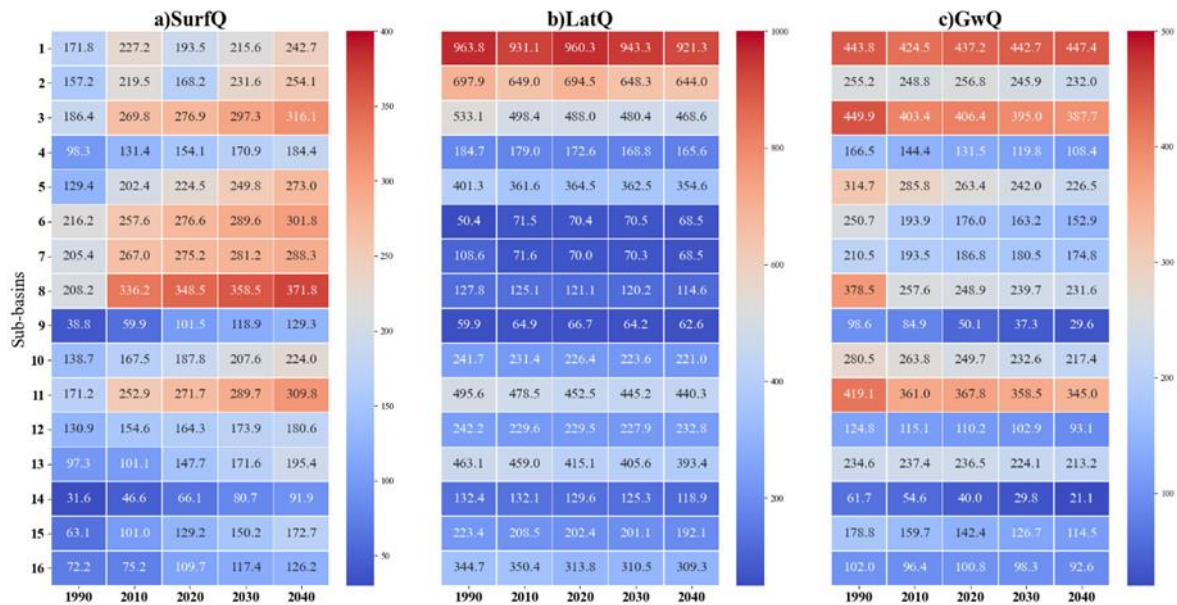
465 **Fig. 16.** Intra-annual variation of a) SurfQ b) LatQ and c) GwQ in different period.

466 With the continuous increase, the minimum-maximum range of surface Q annually is projected
 467 to get further wider in the future. The maximum surface Q and lateral Q will occur in August
 468 while the groundwater Q is predicted to peak in September. Similarly, groundwater Q shows
 469 decreasing trend with time as depicted in **Fig.16c**.

470 *5.2.3 Water-balance change analysis under the present and future landuse at the basin level*

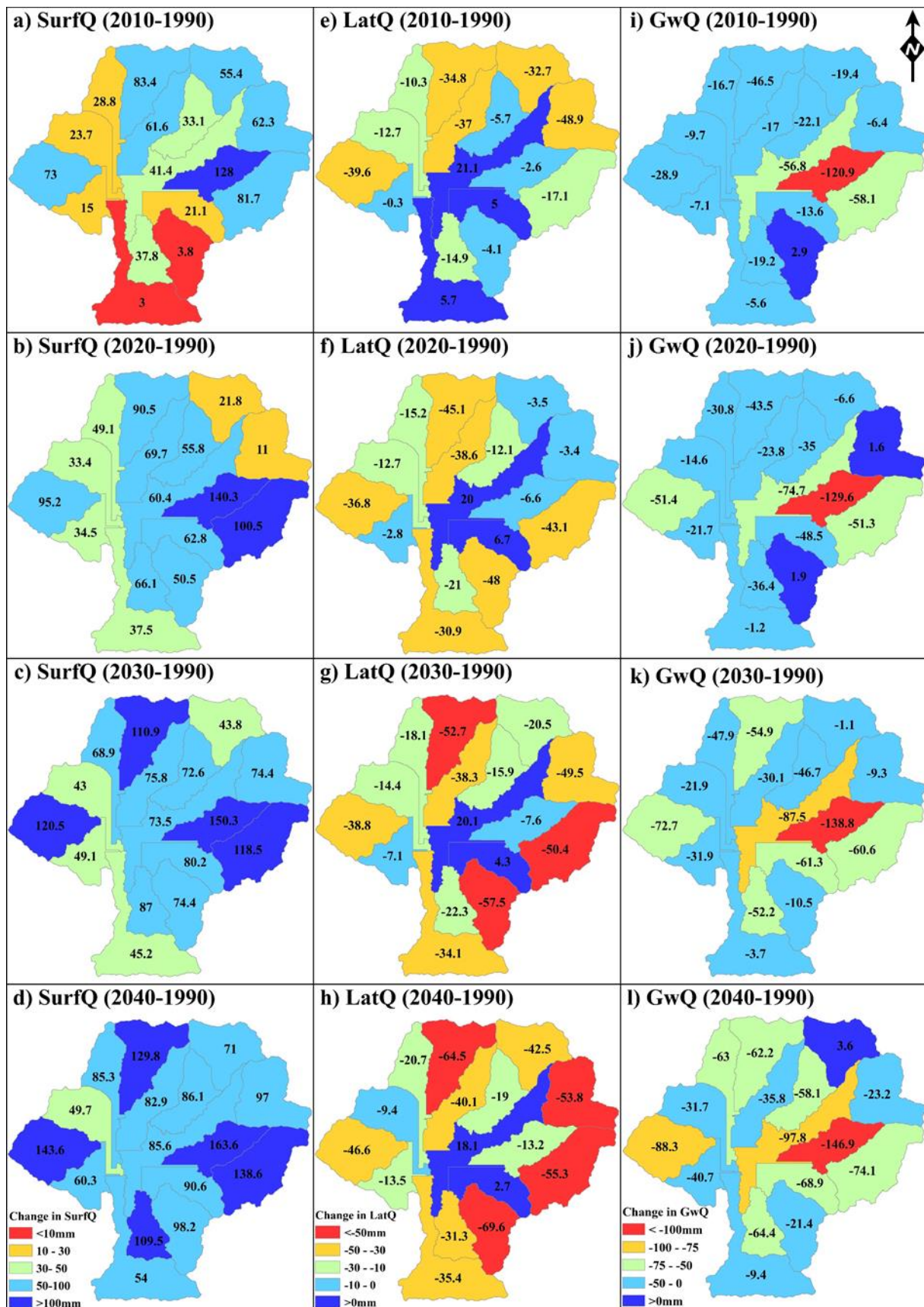
471 It is recognized that the effect of landuse change on the water-balance is more pronounced at
 472 the subbasin scale. It is therefore crucial to identify the potential areas impacted by landuse
 473 change for prioritizing water-management plans. The overall effect of landuse on different
 474 water-balance component may be nullified by each other at the basin scale. So, the actual picture
 475 of the changes within the basin may not be understood clearly. Hence, to better understand the
 476 actual effect on water-balance and water availability, the analysis should be performed at the

477 sub-basin level. In this section, the change in the water-balance component corresponding to
 478 the change in different landuse types in each sub-basin is quantified and analyzed.



479
 480 **Fig. 17.** Subbasin wise variation of a) SurfQ b) LatQ and c) GwQ for different period.

481 **Fig.17** portray the subbasin wise annual water-balance components surface runoff, lateral Q and
 482 the groundwater Q at different time period. The surface runoff in **Fig. 17(a)** shows consistent
 483 increase from the past to the future scenario. The increase in surface runoff is higher for those
 484 subbasins which are yet to be urbanized in comparison to those which are already highly
 485 urbanized. For instance, the surface runoff increased by nearly two folds in subbasin 4 (from 98
 486 to 184mm), subbasin 5 (from 129mm to 273mm), also 13, 14 and 15 while in subbasin 6, it
 487 increased from 216mm to 301mm and in subbasin 7, it increased from 205mm to 288mm. The
 488 change in landuse and the urbanization level of these subbasins can be seen in **Fig. 10**. This
 489 shows that the future impact of urbanization will be felt greater in subbasins that are least
 490 urbanized at present. The increase in surface runoff will likely increase the flash floods and
 491 inundation extent in the future. Similarly, the groundwater component showed a consistent
 492 decline from past to the future scenario as depicted in **Fig. 17(c)**. The decline is relatively greater
 493 in smaller subbasins like 9, 10, 11, 15, etc. Subbasin 1 is exception which is due to the fact that
 494 the landuse projection shows no built-up areas in the future too. The only transition is from
 495 forest to the agricultural areas due to which a slight increase in groundwater component is
 496 observed in subbasin 1. The sub-basin wise variation in lateral Q component as demonstrated
 497 in **Fig. 17(b)**, in general, resembled the groundwater Q pattern. However, the change in the
 498 lateral Q was relatively smaller in comparison to the groundwater Q.

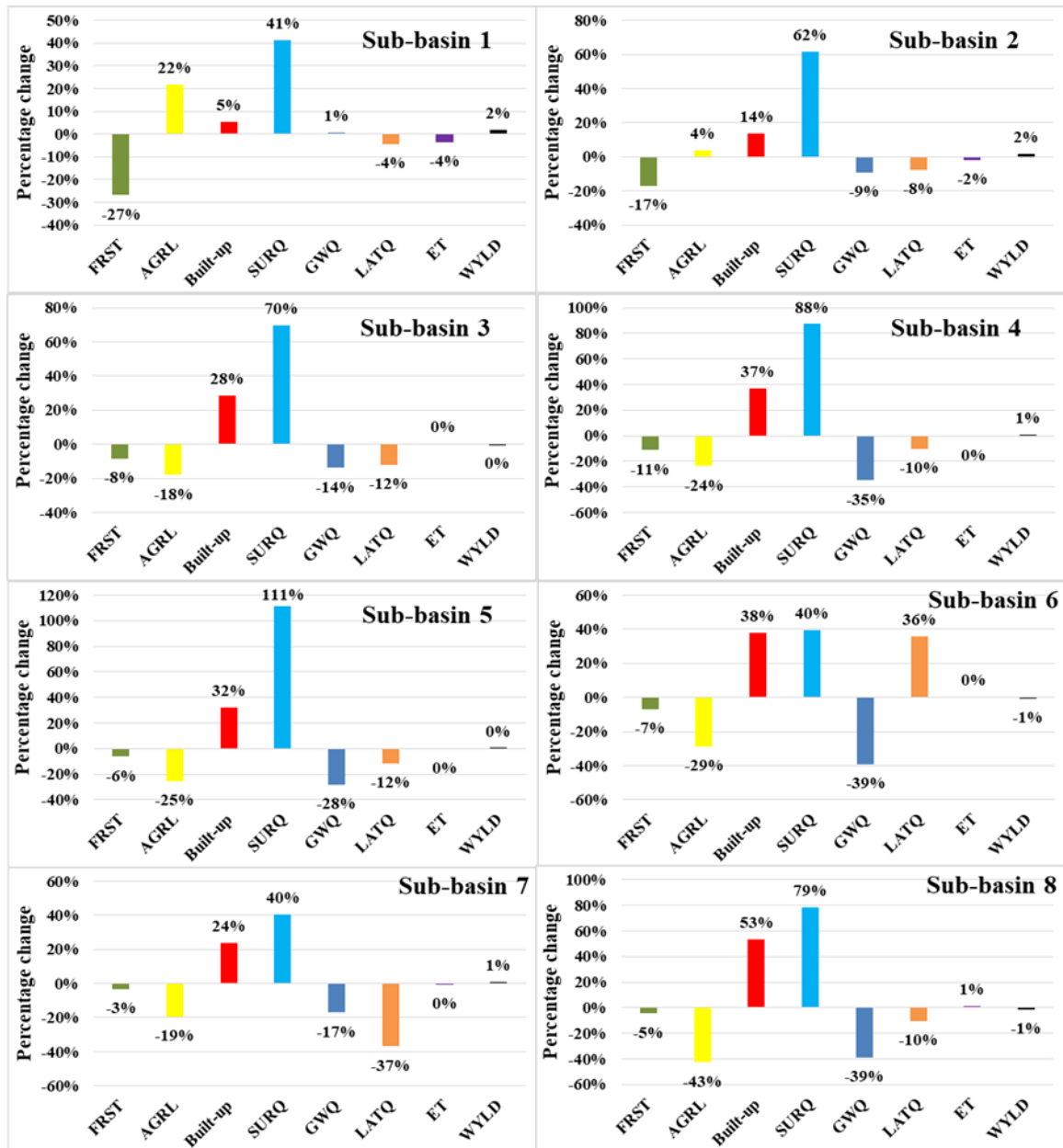


499

500 **Fig. 18.** Subbasin wise change in a) SurfQ b) LatQ and c) GwQ for different decade.

501 The spatial distribution of the actual change (increasing: +ve or decreasing: -ve) in surfQ, latQ

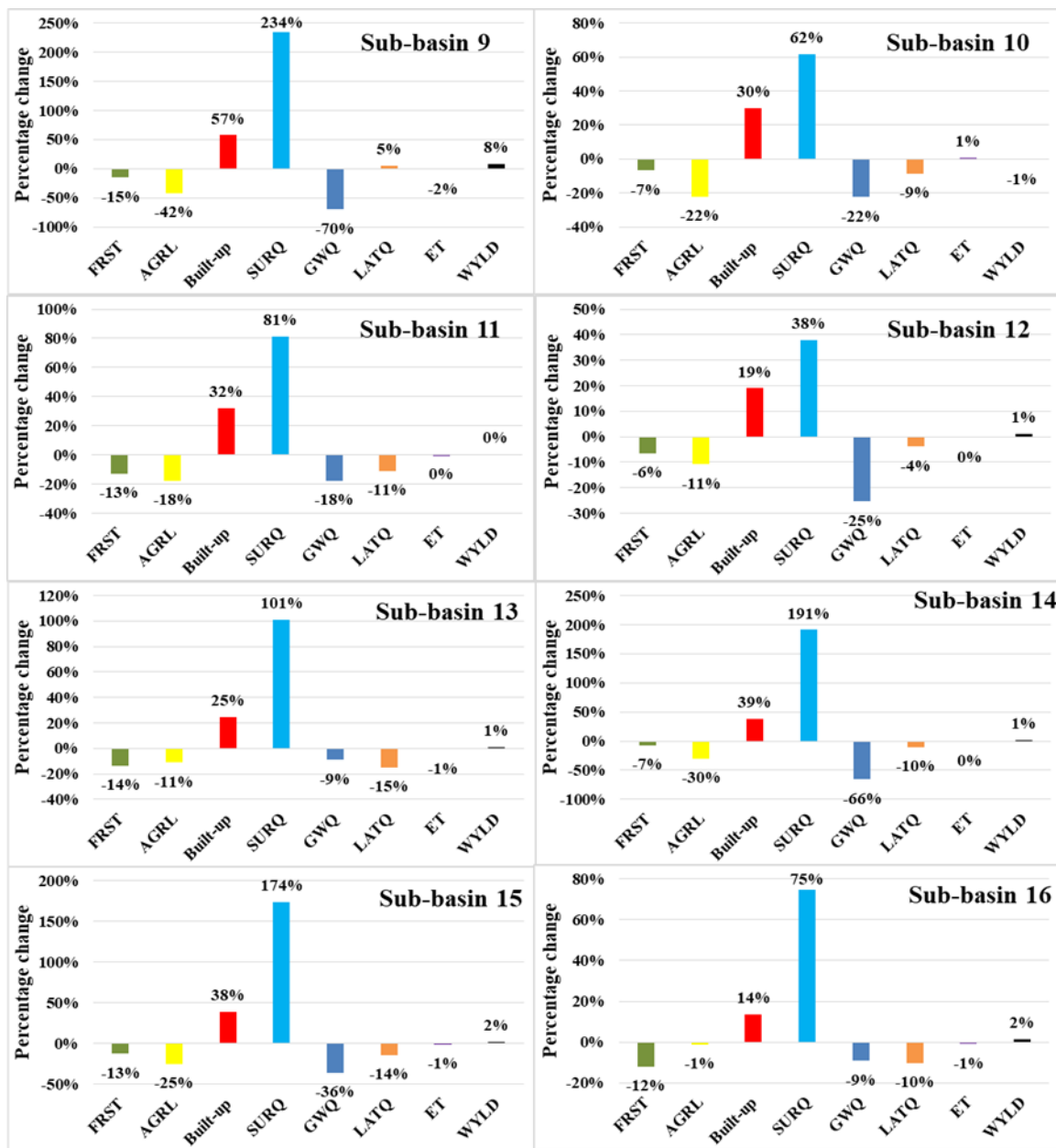
502 and gwQ relative to the baseline scenario is illustrated in **Fig. 18 (a-l)**. We found that the amount
 503 of changes was greater during the period 1990-2010. It is because the major landuse change
 504 also occurred during this period. Among all the subbasins, the surface runoff component in **Fig.**
 505 **18 (a-d)** is projected to increase between 54mm to164mm in 2040 relative to the baseline
 506 scenario of 1990. On the other hand, the lateral Q and the groundwater Q component is likely
 507 to decrease in majority of the subbasins. The lateral Q is expected to decrease between the range
 508 of 10mm to 70mm while the groundwater Q will decline by 10mm to 147mm annually.



509
 510 **Fig. 19.** Projected change in the landuse and different water-balance components for 2040 with
 511 reference to the baseline scenario for subbasin 1-8 (-ve: decrease and +ve: increase)
 512

513 In order to further understand the relation between the landuse change and the corresponding

514 change in water balance component for each sub-basin, the percentage change in landuse types
 515 and water-balance components are plotted in **Fig. 19** and **Fig. 20** for each sub-basins. The
 516 percentage increase in built-up areas ranged from little over 5% to more than 50% while the
 517 increase in surface run-off ranged from about 40% to over 200%. Generally, the percentage
 518 increase in surface run-off was higher for those sub-basins where the built-up area increased.
 519 However, the relation was not linear. For example, surface runoff increased by 234% in sub-
 520 basin 9 (**Fig.20**) in which the built-up area had increased by 57%. But in sub-basin 8 in **Fig.19**,
 521 the percentage change in surface-runoff was only 79% where the built-up area had increased by
 522 53%. This suggest that each hydrological process in a sub-basin is affected by different other
 523 processes. Therefore, it will not always be reasonable to find the one is to one relation.



524
 525 **Fig. 20.** Projected change in the landuse and different water-balance components for 2040 with

526 reference to the baseline scenario for subbasin 9-16 (-ve indicate decrease and +ve indicate
527 increase)
528 Similarly, the decline in groundwater discharge varied from 9% to 70%. The groundwater
529 discharge depends on the pervious cover of the land. Conversion from forest and agriculture to
530 the built-up areas will increase the impervious cover and hence reduces the permeability of the
531 surface. Consequently, the groundwater discharge will decrease. The maximum decline in the
532 groundwater discharge also occurred in sub-basin 9 corresponding to a maximum increase of
533 built-up areas. However, as with the surface run-off, the relation is not linear between the
534 percentage increase of the surface runoff and the built-up areas.

535 **6. CONCLUSIONS**

536 The current study evaluated the water-balance dynamics of the most rapidly urbanizing KVV
537 of Nepal under the past, present and the future landuse scenario. The isolated impact of landuse
538 change was assessed keeping the same climatic conditions for all scenarios. The results and
539 analysis clearly indicated that the rapid urbanization will significantly alter the water-balance
540 components of the study watershed that is already reeling under the water-stress. Projection of
541 landuse revealed that near-about 50% of the total area of KVV will be covered by built-up zone
542 by the year 2040. The increase in the built-up area is compensated mainly by agriculture areas
543 and the forest areas which will have further implications on the multiple ecosystem services.
544 Surface runoff is expected to increase in the future scenario of 2040 by nearly 100mm of which
545 almost 50% (48mm) was found to increase between 1990 and 2010. This will likely have a
546 tremendous impact on the flooding intensity and the extent of inundation within the basin.
547 Another important component, the groundwater discharge which form a basis of daily water
548 consumption in the study watershed is also predicted to decline and that too, without
549 considering the water extraction from the tanker industries. The decline was relatively greater
550 in smaller subbasins. The study also revealed that the response of the subbasins to the landuse
551 change is not necessarily the same for each subbasins rather it depends on the initial landuse
552 distribution of the subbasin. The response was sharper for those subbasins which are yet to be
553 urbanized in comparison to those which are already highly urbanized. The quantification of the
554 changes of different water-balance components revealed that the impact of urbanization on
555 water-balance will be felt greater at the subbasin level. The spatio-temporal distribution of the
556 projected changes in the landuse and the consequent water-balance components at the subbasin
557 level is believed to provide useful information to the policy makers and the related stakeholders
558 to prioritize and formulate the suitable interventions, both soft and hard, to subdue the adverse

559 impact.

560

561 **References**

562 Abbaspour, K.C., Yang, J., Maximov, I., Siber, R., Bogner, K., Mieleitner, J., Zobrist, J.,
563 Srinivasan, R., 2007. Modelling hydrology and water quality in the pre-alpine/alpine Thur
564 watershed using SWAT. *J. Hydrol.* 333, 413–430.
565 <https://doi.org/10.1016/j.jhydrol.2006.09.014>

566 Aboelnour, M., Gitau, M.W., Engel, B.A., 2019. Hydrologic response in an urban watershed as
567 affected by climate and land-use change. *Water (Switzerland)* 11, 1–23.
568 <https://doi.org/10.3390/w11081603>

569 Anand, J., Gosain, A.K., Khosa, R., 2018. Prediction of land use changes based on Land Change
570 Modeler and attribution of changes in the water balance of Ganga basin to land use change
571 using the SWAT model. *Sci. Total Environ.* 644, 503–519.
572 <https://doi.org/10.1016/j.scitotenv.2018.07.017>

573 Ansari, T.A., Katpatal, Y.B., Vasudeo, A.D., 2016. Spatial evaluation of impacts of increase in
574 impervious surface area on SCS-CN and runoff in Nagpur urban watersheds, India. *Arab.*
575 *J. Geosci.* 9. <https://doi.org/10.1007/s12517-016-2702-5>

576 Arnold, J.G., Srinivasan, R., Mutiah, R.S., Williams, J.R., 1998. Large area hydrologic
577 modeling and assessment Part I: Model development. *J. Am. Water Resour. Assoc.* 34, 73–
578 89. <https://doi.org/10.1111/j.1752-1688.1998.tb05961.x>

579 Baker, T.J., Miller, S.N., 2013. Using the Soil and Water Assessment Tool (SWAT) to assess
580 land use impact on water resources in an East African watershed. *J. Hydrol.* 486, 100–111.
581 <https://doi.org/10.1016/j.jhydrol.2013.01.041>

582 Bhusal, R., 2019. Thirsty Kathmandu waits for water that never arrives [WWW Document].
583 URL <https://www.thethirdpole.net/en/climate/kathmandu-water-crisis/>

584 CBS, 2012. Central Bureau of Statistics. Nepal.

585 Cibin, R., Sudheer, K.P., Chaubey, I., 2010. Sensitivity and identifiability of stream flow
586 generation parameters of the SWAT model. *Hydrol. Process.* 24, 1133–1148.
587 <https://doi.org/10.1002/hyp.7568>

588 D. N. Moriasi, J. G. Arnold, M. W. Van Liew, R. L. Bingner, R. D. Harmel, T. L. Veith, 2007.
589 Model Evaluation Guidelines for Systematic Quantification of Accuracy in Watershed
590 Simulations. *Trans. ASABE* 50, 885–900. <https://doi.org/10.13031/2013.23153>

591 Dijkshoorn, K., Jan Huting, 2009. Soil and Terrain database for Nepal, Report 2009/01. ISRIC

592 – World Soil Information, Wageningen.

593 Eastman, J.R., 2016. TerrSet Geospatial Monitoring and Modelling System Manual.

594 Fang, D., Hao, L., Cao, Z., Huang, X., Qin, M., Hu, J., Liu, Y., Sun, G., 2020. Combined effects
595 of urbanization and climate change on watershed evapotranspiration at multiple spatial
596 scales. *J. Hydrol.* 587, 124869. <https://doi.org/10.1016/j.jhydrol.2020.124869>

597 Gashaw, T., Tulu, T., Argaw, M., Worqlul, A.W., 2018. Modeling the hydrological impacts of
598 land use/land cover changes in the Andassa watershed, Blue Nile Basin, Ethiopia. *Sci.*
599 *Total Environ.* 619–620, 1394–1408. <https://doi.org/10.1016/j.scitotenv.2017.11.191>

600 Gupta, H.V., Kling, H., Yilmaz, K.K., Martinez, G.F., 2009. Decomposition of the mean squared
601 error and NSE performance criteria: Implications for improving hydrological modelling.
602 *J. Hydrology* 377, 80–91.

603 Gupta, H.V., Sorooshian, S., Yapo, P.O., 1999. STATUS OF AUTOMATIC CALIBRATION
604 FOR HYDROLOGIC MODELS: COMPARISON WITH MULTILEVEL EXPERT
605 CALIBRATION 4, 135–143.

606 Hamad, R., Balzter, H., Kolo, K., 2018. Predicting land use/land cover changes using a CA-
607 Markov model under two different scenarios. *Sustain.* 10, 1–23.
608 <https://doi.org/10.3390/su10103421>

609 ICIMOD, 2013. Land cover of Nepal 2010.

610 Ishtiaque, A., Shrestha, M., Chhetri, N., 2017. Rapid urban growth in the kathmandu valley,
611 nepal: Monitoring land use land cover dynamics of a himalayan city with landsat imageries.
612 *Environ. - MDPI* 4, 1–16. <https://doi.org/10.3390/environments4040072>

613 Jothityangkoon, C., Sivapalan, M., Farmer, D.L., 2001. Process controls of water balance
614 variability in a large semi-arid catchment: Downward approach to hydrological model
615 development. *J. Hydrol.* 254, 174–198. [https://doi.org/10.1016/S0022-1694\(01\)00496-6](https://doi.org/10.1016/S0022-1694(01)00496-6)

616 Karki, S., 2012. Application of Uncertainty Analysis Techniques To Swat Model : A Case Study
617 of West Seti River Basin, Nepal. Institute of Engineering, Tribhuvan University.

618 Kim, K.B., Kwon, H.H., Han, D., 2018. Exploration of warm-up period in conceptual
619 hydrological modelling. *J. Hydrol.* 556, 194–210.
620 <https://doi.org/10.1016/j.jhydrol.2017.11.015>

621 Krause, P., Boyle, D.P., Bäse, F., 2005. Comparison of different efficiency criteria for
622 hydrological model assessment. *Adv. Geosci.* 5, 89–97. [https://doi.org/10.5194/adgeo-5-](https://doi.org/10.5194/adgeo-5-89-2005)
623 [89-2005](https://doi.org/10.5194/adgeo-5-89-2005)

624 Kumar, N., Tischbein, B., Kusche, J., Beg, M.K., Bogardi, J.J., 2017. Impact of land-use change
625 on the water resources of the Upper Kharun Catchment, Chhattisgarh, India. *Reg. Environ.*

626 Chang. 17, 2373–2385. <https://doi.org/10.1007/s10113-017-1165-x>

627 Kundu, S., Khare, D., Mondal, A., 2017. Past, present and future land use changes and their
628 impact on water balance. *J. Environ. Manage.* 197, 582–596.
629 <https://doi.org/10.1016/j.jenvman.2017.04.018>

630 Lamichhane, S., Shakya, N.M., 2019a. Integrated assessment of climate change and land use
631 change impacts on hydrology in the Kathmandu Valley watershed, Central Nepal. *Water*
632 (Switzerland) 11. <https://doi.org/10.3390/w11102059>

633 Lamichhane, S., Shakya, N.M., 2019b. Alteration of groundwater recharge areas due to land
634 use/cover change in Kathmandu Valley, Nepal. *J. Hydrol. Reg. Stud.* 26, 100635.
635 <https://doi.org/10.1016/j.ejrh.2019.100635>

636 McCuen, R.H., Knight, Z., Cutter, A.G., 2006. Evaluation of the Nash–Sutcliffe Efficiency
637 Index. *J. Hydrol. Eng.* 11, 597–602. [https://doi.org/10.1061/\(asce\)1084-0699\(2006\)11:6\(597\)](https://doi.org/10.1061/(asce)1084-0699(2006)11:6(597))

639 Muzzini, E., Aparicio, G., 2013. Urban Growth and Spatial Transition in Nepal, Urban Growth
640 and Spatial Transition in Nepal. <https://doi.org/10.1596/978-0-8213-9659-9>

641 Neitsch, S.L., Arnold, J.G., Kiniry, J.R., Williams, J.R., 2011. Soil & Water Assessment Tool
642 Theoretical Documentation Version 2009. Texas Water Resour. Inst. 1–647.

643 Pandey, V.P., Chapagain, S.K., Kazama, F., 2010. Evaluation of groundwater environment of
644 Kathmandu Valley. *Environ. Earth Sci.* 1329–1342. <https://doi.org/10.1007/s12665-009-0263-6>

645

646 Pokhrel, B.K., 2018. Impact of land use change on flow and sediment yields in the Khokana
647 outlet of the Bagmati River, Kathmandu, Nepal. *Hydrology* 5.
648 <https://doi.org/10.3390/hydrology5020022>

649 Sharma, C.K., 1987. River Systems of Nepal.

650 Shrestha, M., Acharya, S.C., 2020. Assessment of historical and future land-use–land-cover
651 changes and their impact on valuation of ecosystem services in Kathmandu Valley, Nepal.
652 *L. Degrad. Dev.* <https://doi.org/10.1002/ldr.3837>

653 Shrestha, S., Neupane, S., Mohanasundaram, S., Pandey, V.P., 2020. Mapping groundwater
654 resiliency under climate change scenarios : A case study of Kathmandu Valley , Nepal.
655 *Environ. Res.* 183, 109149. <https://doi.org/10.1016/j.envres.2020.109149>

656 Sinha, R.K., Eldho, T.I., 2018. Effects of historical and projected land use/cover change on
657 runoff and sediment yield in the Netravati river basin, Western Ghats, India. *Environ. Earth*
658 *Sci.* 77, 1–19. <https://doi.org/10.1007/s12665-018-7317-6>

659 Thapa, B.R., Ishidaira, H., Pandey, V.P., Bhandari, T.M., Shakya, N.M., 2018. Evaluation of

660 water security in Kathmandu Valley before and after water transfer from another basin.
661 Water (Switzerland) 10, 1–12. <https://doi.org/10.3390/w10020224>

662 Thapa, B.R., Ishidaira, H., Pandey, V.P., Shakya, N.M., 2017. A multi-model approach for
663 analyzing water balance dynamics in Kathmandu Valley, Nepal. *J. Hydrol. Reg. Stud.* 9,
664 149–162. <https://doi.org/10.1016/j.ejrh.2016.12.080>

665 United Nations, 2018. World Urbanization Prospects, Demographic Research.

666 Wagner, P.D., Kumar, S., Schneider, K., 2013. An assessment of land use change impacts on the
667 water resources of the Mula and Mutha Rivers catchment upstream of Pune, India. *Hydrol.*
668 *Earth Syst. Sci.* 17, 2233–2246. <https://doi.org/10.5194/hess-17-2233-2013>

669 Wakode, H.B., Baier, K., Jha, R., Azzam, R., 2018. Impact of urbanization on groundwater
670 recharge and urban water balance for the city of Hyderabad, India. *Int. Soil Water Conserv.*
671 *Res.* 6, 51–62. <https://doi.org/10.1016/j.iswcr.2017.10.003>

672 Winchell, M., Srinivasan, R., Di Luzio, M., Arnold, J., 2013. ArcSWAT Interface For
673 SWAT2012: User’s Guide. Texas Agric. Exp. Stn. United States Dep. Agric. Temple, TX.
674 464.

675 Woldesenbet, T.A., Elagib, N.A., Ribbe, L., Heinrich, J., 2017. Hydrological responses to land
676 use/cover changes in the source region of the Upper Blue Nile Basin, Ethiopia. *Sci. Total*
677 *Environ.* 575, 724–741. <https://doi.org/10.1016/j.scitotenv.2016.09.124>

678 Wu, F., Zhan, J., Su, H., Yan, H., Ma, E., 2015. Scenario-Based Impact Assessment of Land
679 Use/Cover and Climate Changes on Watershed Hydrology in Heihe River Basin of
680 Northwest China. *Adv. Meteorol.* 2015. <https://doi.org/10.1155/2015/410198>

681 Zhou, F., Xu, Y., Chen, Y., Xu, C.Y., Gao, Y., Du, J., 2013. Hydrological response to
682 urbanization at different spatio-temporal scales simulated by coupling of CLUE-S and the
683 SWAT model in the Yangtze River Delta region. *J. Hydrol.* 485, 113–125.
684 <https://doi.org/10.1016/j.jhydrol.2012.12.040>

685